気象庁欧文海洋報告

第22巻 第2号

THE OCEANOGRAPHICAL MAGAZINE

Vol. 22 No. 2

CONTENTS

SAGI, T.: On the distribution of nitrate nitrogen in the western North Pacific Ocean 63

AKAMATSU, H.: The ocean data station buoys of the Japan Meteorological Agency 75

HAYASHI, S., H. TAKANO and A. YAMASHITA: Maritime meteorological summary of western North Pacific Ocean in the winters of 1967, 1968 and 1969 95

LIBRARY
MAY 25 1971
FISH & WILDLIFE SERVICE

Published by the Japan Meteorological Agency
December, 1970

The Oceanographical Magazine
Vol. 22, No. 2, pp. 63 to 74, December 1970

On the distribution of nitrate nitrogen in the western North Pacific Ocean

Takeshi SAGI

Japan Meteorological Agency

(Received August 31, 1970)

Abstract: On the three cruises of the R.V. *Ryofu Maru* in 1969, nitrate contents in sea water, including smaller amount of nitrite, were determined by the method using copperized cadmium filings to reduce nitrate to nitrite. The measurements were made mainly on three long sections along 155°E (20°–48°N), 137°E (1°S–33°30′ N), 130°E (1°–20°N), and in the Japan Sea. On the basis of results of measurements, the distribution of nitrate and the ratio of nitrate to phosphate are discussed.

The contents of nitrate in the surface water are below 1.0 μg·at/l in most of the observed areas except the Oyashio region. In the Oyashio region, the remarkably higher contents than 25 μg·at/l are found in the surface water. The maximum contents of nitrate ranging from 25 to 45 μg·at/l between 400m and 2000m are observed usually below the oxygen-minimum layer. In the equatorial region, south of about 15°N, however, the layer of the maximum contents of nitrate does not coincide with that of oxygen-minimum. In waters of the Kuroshio, the subtropics and the equatorial region, the maximum values are a little higher than 40 μg·at/l and differences in concentration among regions are very small. In the Japan Sea, maximum values are about 25 μg·at/l, which are much less than those in the Pacific.

The atomic ratios of nitrate to phosphate range approximately from 12 to 15. The higher ratios more than 14 are found in deep waters of the Oyashio region and the equatorial region. On the other hand, the ratio for oxidized part is found to be nearly constant value of 15.

1. Introduction

Nitrogen, phosphorus and silicon in sea water are fundamental nutrient materials for living matters. They are also useful for the analysis of water masses (VACCARO, 1965; LISS, 1969). Because of the readiness of determinations, phosphorus and silicon are often measured routinely on oceanographic cruises, and the general features of these elements in the Pacific have been investigated to some extent (KITAMURA and SAGI, 1964; ARMSTRONG, 1965). On the contrary, determination of nitrate in sea water was difficult especially under shipboard conditions. There have been

very few data available for nitrate in the western North Pacific. In recent years, a reliable technique for nitrate analysis has been developed by WOOD, ARMSTRONG and RICHARDS (1967).

The inorganic nitrogen compounds in sea water were determined on the cruises of the R.V. *Ryofu Maru* in 1969. As a result, it is found that the distribution of nitrogen compounds is somewhat complicated as compared with that of phosphate, although the most part of nitrogen in sea water may be incorporated in nitrate except near the surface. In this paper, the general pattern of nitrate distribution in relation to the water circulation is described.

REDFIELD (1934) found that the ratios of nitrogen to phosphorus in the sea is generally close to 15 : 1 by atoms. COOPER (1938) showed that the ratios vary with geographical positions. In the western North Pacific, it is expected that by knowing the distribution of nitrate and the atomic ratio of nitrate to phosphate the deep water may be classified into some characteristic water masses.

2. Samples and method of analysis

Three cruises of the R.V. *Ryofu Maru* were carried out in the western North Pacific and the Japan Sea in 1969. The measurements of nitrate were made mainly on the three long sections along 155°E (20°—48°N), 137°E (1°S—33°30′N), 130°E, (1°—20°N), and in the Japan Sea (Fig. 1).

Analyses of nitrate were carried out using copperized cadmium filings to reduce nitrate to nitrite, followed by diazotization and development of the azo dye with N-(1-naphthyl)-ethylenediamine (WOOD, ARMSTRONG and RICHARDS, 1967). A spectrophotometer (Hitachi Perkins-Elmer 139) with a quartz cell of 1 cm path length was used for the measurements.

3. Results and discussion

3-1 Vertical distribution

The northern branch of the Kuroshio Extension is mixed with Oyashio water in the sea east of Honshu, Japan. Therefore, the vertical distribution along the 155°E meridian is convenient to find out the characteristic of two main water masses. As shown in Fig. 2, the Kuroshio front and the Oyashio front are situated at about 34°N and 40°N respectively. In waters near the surface, low contents less

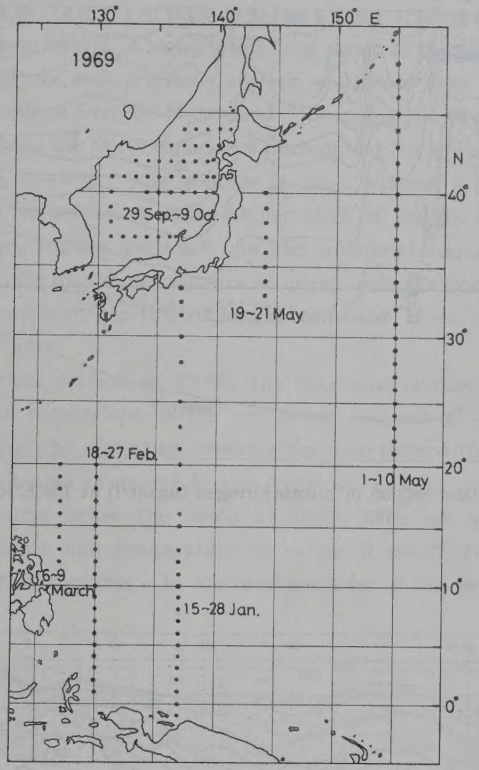

Fig. 1. Location of sampling positions on the cruises of the R.V. *Ryofu Maru* in 1969.

than 1 μg·at/l are observed in the sea south of the Kuroshio front, while the remarkably higher contents than 25 μg·at/l are found in the Oyashio region. At about 45°N, nitrate contents more than 45 μg·at/l are observed from about 400 m down to the depth of about 800m. The maximum content of 48 μg·at/l is recorded in the Oyashio region at around the depth of 800m. In the Oyashio region, additional nitrate seems to be carried downward by the sinking of organisms. Higher contents than 40 μg·at/l are present between the depth of 800m and 2500m.

A meridional section at 137°E from Japan to New Guinea is shown in Fig. 3. In the section, nitrate is depleted near the surface and rises to the maximum at

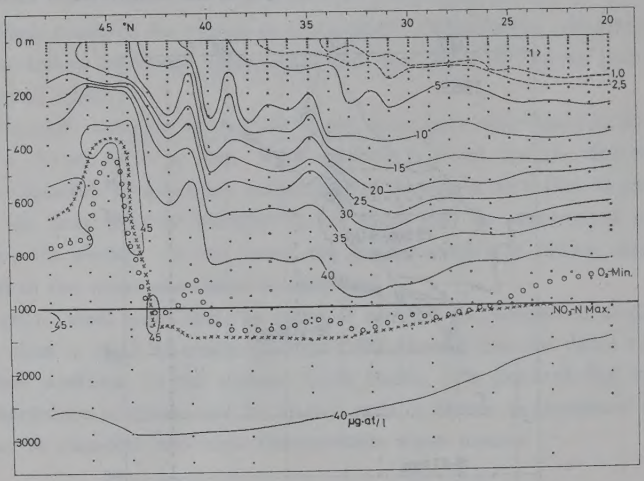

Fig. 2. Vertical section of nitrate-nitrogen ($\mu g \cdot at/l$) at 155°E in May 1969.

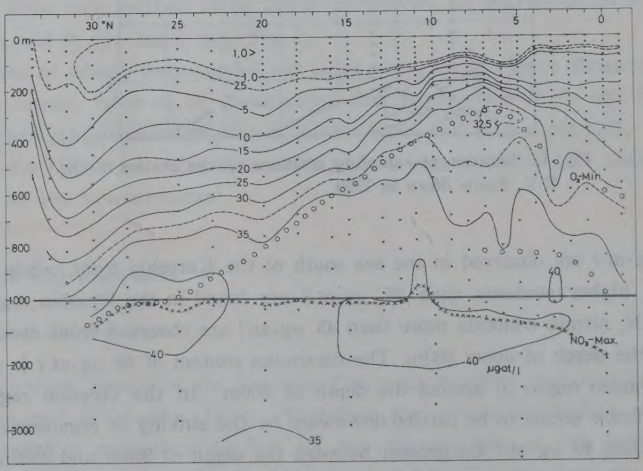

Fig. 3. Vertical section of nitrate-nitrogen ($\mu g \cdot at/l$) at 137°E in January 1969.

moderate depth (1000～1500m) and then decreases a little. The nitrate content is relatively uniform in deep waters. A sharp gradient at about 33°N indicates the Kuroshio water. The contour becomes gradually shallow southward from 30°N to 20°N and becomes steeply shallow from 20°N to about 7°N in the North Equatorial Current. The boundary between the North Equatorial Current and Equatorial Counter Current is located at about 7°—8°N. The contour is most shallow in this area. In this section, maximum values are a little higher than 40 μg·at/l and differences in concentration among regions are small. In the equatorial region south of about 15°N, the layer of the maximum contents of nitrate does not coincide with that of the oxygen minimum layer. In this region, it seems that there are two minima of oxygen content (Fig. 4).

In the meridional section at 130°E, the maximum contents are less than 40 μg·at/l (Fig. 5). In comparison of the meridional sections at 155°E, 137°E and 130°E, it is seen that the maximum contents decrease toward the west.

A typical distribution of nitrate in the Japan Sea is shown in Fig. 6. In the Japan Sea, the waters below the depth of about 300m are quite homogeneous with respect to salinity and temperature (σ_t range 27.30—27.37). They are relatively low in nitrate contents. In the western sides of the Japan Sea, a nitrate

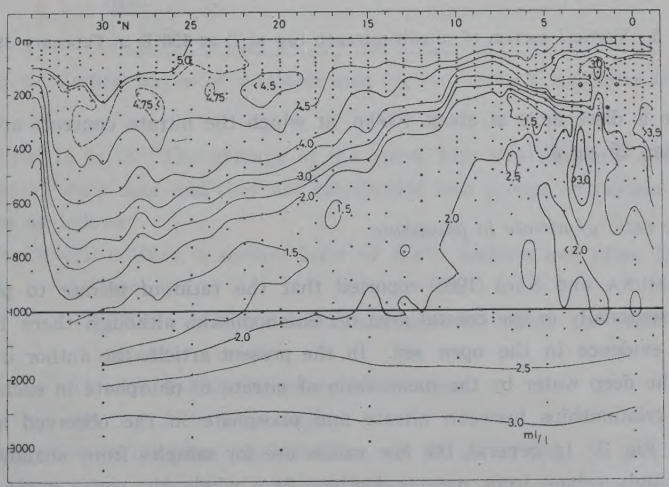

Fig. 4. Vertical section of oxygen content (ml/l) at 137°E in January 1969.

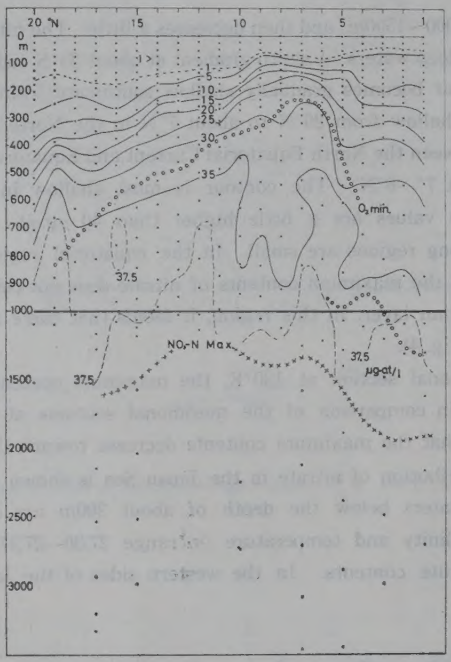

Fig. 5. Vertical section of nitrate-nitrogen (μg·at/l) at 130°E in February 1969.

maximum is discernible at about 1000m, at which the nitrate contents are a little higher than 25 μg·at/l.

3-2 The ratio of nitrate to phosphate

KITAMURA and SAGI (1965) reported that the ratio of nitrate to phosphate changed seasonally in the coastal area off Shionomisaki, although there has been no such evidence in the open sea. In the present article, the author intends to classify the deep water by the mean ratio of nitrate to phosphate in each area.

The relationships between nitrate and phosphate in the observed areas are shown in Fig. 7. In general, the low values are for samples from shallow depths and the high values from greater depths. As a whole, the ratios range approxi-

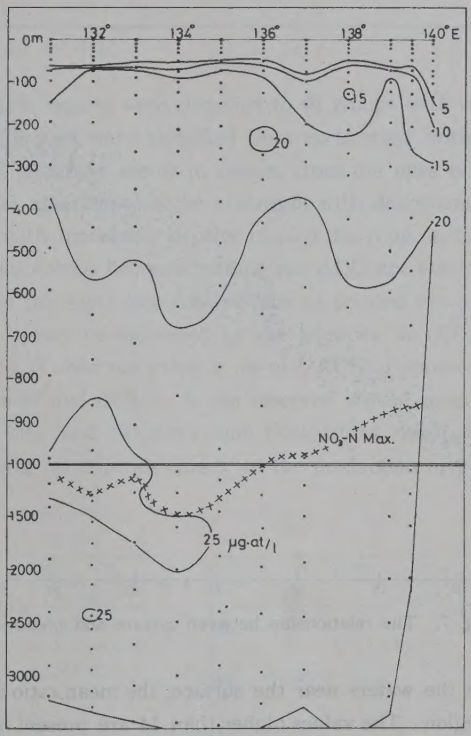

Fig. 6. Vertical section of nitrate-nitrogen ($\mu g \cdot at/l$) at 41°N in October 1969.

mately from 12 to 15. The average of the ratios with the standard deviations is calculated for each area and they are sub-divided into groups by certain arbitrary conditions as follows:

in the Pacific—(1) 0–100m, a surface layer of fairly uniform and often low nitrate contents.

(2) 100m—σ_t 27.0, transitional region in which the ratio increases rapidly.

(3) σ_t 27.0–27.5, the intermediate water.

(4) $> \sigma_t$ 27.5, deep water.

in the Japan Sea—(1) 0–100m. (2) 100–300m. (3) 300 m—0_2 min. (4) $> 0_2$ min.

The ratios have a tendency to increase whereas the dispersions decrease with in-

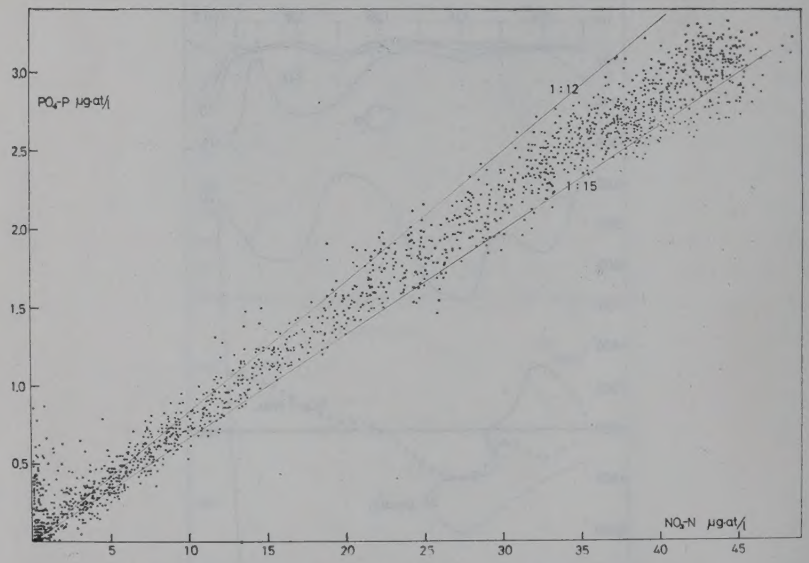

Fig. 7. The relationship between nitrate and phosphate.

creasing depth. In the waters near the surface, the mean ratio is the highest (12.7 : 1) in the Oyashio region. The values higher than 14 are present in the intermediate waters of the Oyashio and the equatorial region (Fig. 8 a, b). The boundaries in the ratio are found in deep waters at about 18°N and 14°N along 137°E and 130°E meridian. The ratio in the Oyashio region is high at all the depths. In deep waters in the subtropical region along 137°E and 130°E meridian, the mean ratios are lower than that of the value along 155°E. It may be supposed that the mean ratios in deep waters are low at the north Philippine basin. Around the Philippines and adjacent area, MEGIA and LAO (1955) found that the ratios close to a mean of 13.5 : 1. A similar value of $13.6 \pm 0.3 : 1$ is shown in the deep water along 130°E meridian (Fig. 8c).

In the Japan Sea, the ratio is relatively low and in waters below a depth of 100m is quite homogeneous (Fig. 8d). In waters near the surface, the ratio is lowest on the south eastern side, which suggests that the nitrate-poor water flows into the Japan Sea.

3–3 Relation of nitrate to AOU

As shown in Fig. 9, waters were classified to 40 groups with respect to density and salinity, and the groups were identified from each other with various marks. The nitrate to AOU diagram seems to consist from the piles of different groups of waters, which seem approximately be arranged, with decreasing salinity toward the upper parts and with increasing density toward the right in the figure. On the whole, the linear relationships between nitrate and AOU are obtained in the water with equal salinity on the same isopicnal surface as pointed out by SUGIURA and YOSHIMURA (1964). It may be expressed by the equation as $(NO_3)_{ob} = 15/3\,AOU + (NO_3)_{res}$ where $(NO_3)_{ob}$ is observed value in $\mu g \cdot at/l$, AOU or apparent oxygen utilization is expressed in ml/l and $(NO_3)_{res}$ is the reserved nitrate proposed by SUGIURA (1965). REDFIELD (1934), and SUGIURA and YOSHIMURA (1964) showed that O : P ratio of oxidative origin corresponds closely to the production of 1 $\mu g \cdot at/l$ of phos-

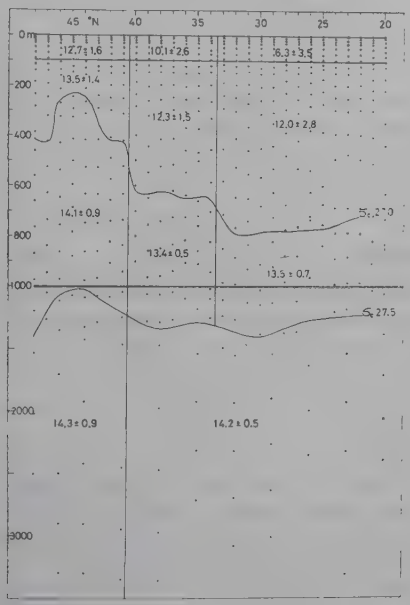

(8–a)

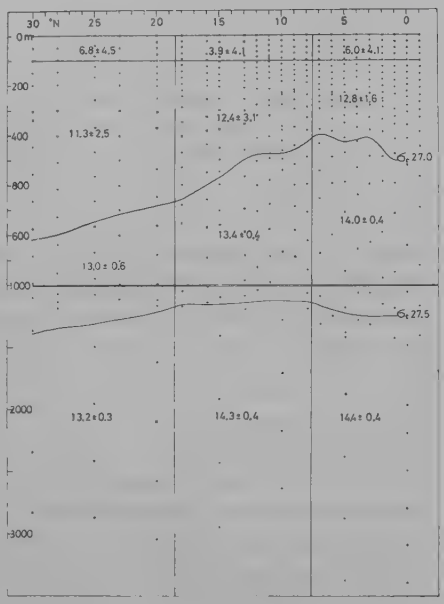

(8–b)

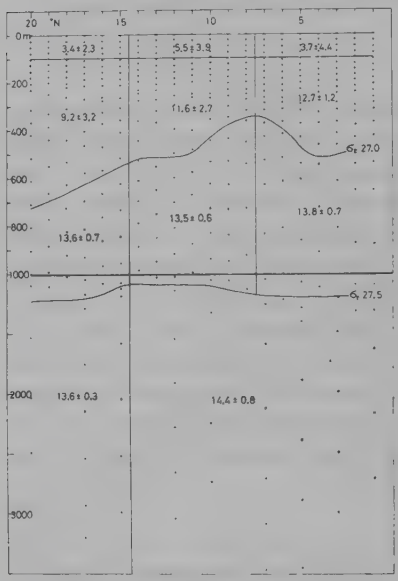

(8-c)

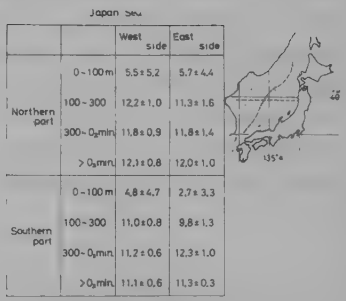

(8-d)

Fig. 8. The average of the ratio N/P in each area with the standard deviation in the vertical section along the longitude of 137°E (a), 155°E (b), 130°E (c), and in the Japan Sea (d).

phate in the consumption of 3 m*l*/*l* of oxygen. In the present data, similar relationship between phosphate and AOU is obtained as $P_{ob} = 1/3\,AOU + P_{res}$. From above two equations, it seems that the ratio of nitrate to phosphate of oxidized part reaches finally a constant value of 15, although the ratio of the observed values varies from 12 to 15.

Acknowledgements

The author wishes to express his hearty thanks to prof. Yasuo MIYAKE, Tokyo Kyoiku University for his kind advice and the critical reading of the manuscript. He also appreciates to Messrs. T. AKIYAMA, H. YOSHIMURA, T. YURA and K. KIMURA, Japan Meteorological Agency, for their cooperation in determinations and critical discussions.

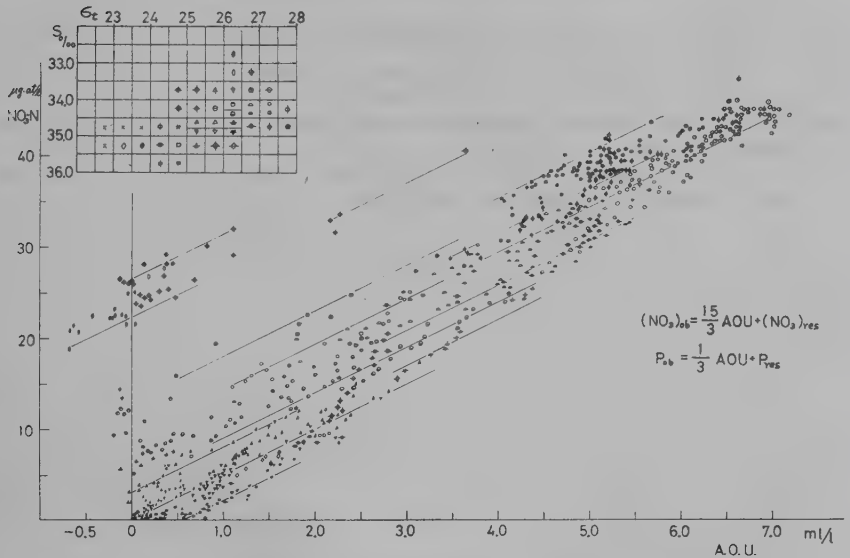

Fig. 9. Nitrate-nitrogen to AOU relation.

References

ARMSTRONG F.A.J. (1965): Silicon, in J.P. RILEY and G. SKIRROW, ed.: Chemical Oceanography, Vol. **1**, 409–435.

COOPER L.H.N. (1938): Redefinition of anomaly of the nitrate-phosphate ratio. *J. mar. biol. Ass. U.K.*, **23**, 171–178.

KITAMURA H. and T. SAGI (1964): On the chemical elements in the sea south of Honshu, Japan. Part 1. *Bull. Kobe Marine Observatory*, **172**, 6–54.

KITAMURA H. and T. SAGI (1965): On the chemical elements in the sea south of Honshu, Japan. Part 2. *Bull. Kobe Marine Observatory*, **174**, 39–55.

LISS P.S. (1969): Reactive silicate concentrations observed in the Irish Sea. *J. mar. biol. Ass. U.K.*, **49**, 577–588.

MEGIA T.G. and R.G. LAO (1955): *Philippine, J. Fish.* **3**, 55. cited from F.A.J. ARMSTRONG (1965): Phosphorus, in J.P. RILEY and G. SKIRROW, ed.: Chemical Oceanography Vol. **1**, 332–364.

REDFIELD A.C. (1934): On the proportions of organic derivatives in sea water and their relation to the composition of plankton. James Johnstone Memorial Volume, Liverpool. 177–192. cited from A.C. REDFIELD, B.H. KETCHUM and F.A. RICHARDS (1963): The influence of organisms on the composition of sea-water, in M.N. HILL, ed.: The Sea. Vol. **2**, 26–77.

SUGIURA Y. and H. YOSHIMURA (1964): Distribution and mutual relation of dissolved oxygen

and phosphate in the Oyashio and the northern part of Kuroshio regions. *J. Oceanogr. Soc. Japan*, **20**, 13–23.

SUGIURA Y. (1965): Distribution of reserved (preformed) phosphate in the Subarctic Pacific region. *Papers in Meteo. and Geophysics*, **15**, 208–215.

VACCARO R. F. (1965): Inorganic nitrogen in sea water, in J. P. RILEY and G. SKIRROW, ed.: Chemical Oceanography, Vol. **1**, 365–404.

WOOD E. D., F. A. J. ARMSTRONG and F. A. RICHARDS (1967): Determination of nitrate in sea water by cadmium-copper reduction to nitrite. *J. mar. biol. Ass. U.K.*, **47**, 23–31.

The Oceanographical Magazine
Vol. 22, No. 2, pp. 75 to 94, December 1970

The ocean data station buoys of the Japan Meteorological Agency

Hideo AKAMATSU

Maizuru Marine Observatory

(Received August 31, 1970)

1. Introduction

The Ocean Data Station Buoys were completed with financial support for research and investigation established by the Science and Technology Agency, for the Japan Meteorological Agency (J.M.A.) Their purpose is to investigate the relationship between the sea and weather, at the polar front in the Japan Sea, as a part of a development plan to investigate the Japan Sea which has been in operation since 1968.

One buoy was completed in 1968 and a second in 1969 as a part of a development program for the J.M.A.. The second one is the present standard.

Between the 16th of May and the 19th of June the No. 1 Buoy and No. 2 Buoy were positioned on the surface in the middle part of the Japan Sea and moored in depths of 1820m and 1800m respectively. The No. 1 Buoy was located at 38°53′N, 133°37′E and the No. 2 Buoy at 39°46′N, 134°32′E.

The Meteorological and Oceanographic Data from these buoys was transmitted 8 times per day (every three hours) to the Maizuru Marine Observatory and the Kiyose Communication Station of the J.M.A. at distances of 500 km and 650 km from the buoys, respectively.

This report presents a brief description of the No. 2 ocean data buoy with emphasis on its meteorological and oceanographic sensors, electronic devices and its data.

2. System configuration

The system comprises two stations namely the buoy at sea which gathers and transmits meteorological and oceanographic data, and a shore station to receive the

data.

The total weight of the buoy is 3.0 tons including ballast and it has an excess buoyancy of about 3.5 tons. The hull has a discus configuration approximately 3.5 m in diameter, 0.5m in depth, drafting a little more than 0.2m of water. It has a 2 m tower for the antenna, meteorological sensors and the beacon (radar reflector and marker lamp).

Radio frequencies* of 4 and 8 MHz, within the WARC bands allocated for collecting meteorological and oceanographic data, are used and switched automatically corresponding to day or night. The data is transmitted to the shore station using these frequencies.

Eleven parameters are measured, namely wind direction, wind speed, barometric pressure, air temperature, water temperature (at five depths), current direction and current speed. The first nine items are transmitted to the shore station in a one minute time cycle. The transmission speed is 50 bauds and a Pulse Duration Modulation (PDM)-Frequency Shift Keyed (FSK) system is used. Magnetic tape is employed for all items including current direction and current speed to record and store the data.

Measurement and transmission of data is done automatically by a crystal clock inside the buoy which may be set to transmit (every hour, every three hours and every six hours with G.M.T. $00^{h}00^{m}$ as the standard time with manual operation).

The antenna is a whip type of about 8 m length and the output power is 25 watts. Range is more than 500 km but may be greater when ionospheric conditions are favourable. This system is used for many kinds of data collection about sea conditions at relatively short distances.

The continuous operation is limited for three months with the Ni-Cd battery capacity. The shore statione employs a power source with capacity to run the time control circuit for 72 hours of continuous main power failure.

3. Buoy station

Fig. 1 shows the No. 2 Buoy at sea, and Fig. 2 shows the configuration of the No. 2 Buoy. The basic block diagram of the buoy station is shown in Fig. 3.

* Frequency utilization is essentially as described in the report of WARC, 1967, and as outlined in the report of the Working Group on Communications, International Oceanographic Commission, UNESCO, which specified six radio bands in the 4, 6, 8, 12, 16 and 22 MHz regions, each having a band-width of 3500 Hz, each 3500 Hz band being divided into ten 300 Hz data channels and two 250 Hz guard bands.

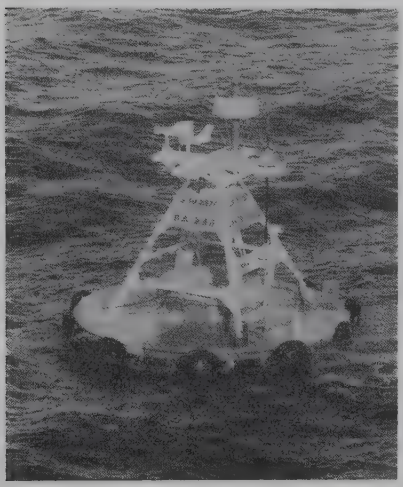

Fig. 1. The Ocean Data Station, No. 2 Buoy at sea.

The primary purpose of the system is to gather meteorological and oceanographic data, store it and transmit it to shore. Equipment in the buoy system consists of the telemetry system, the data acquisition and control system, meteorological and oceanographic sensors, the electric power source and antenna.

3-1 Meteorological and oceanographic sensors of buoy station

(A) Wind direction

(a) By finding true north with a magnetic compass and comparing it with the measured wind direction, wind direction is represented as one of sixteen bearings displayed by a numerical value. A luminous diode and photo-transistors are employed as the tranducing element. Reliability is thus increased by having no moving contacts.

(b) The circuit provides a one minute average of wind direction.

(c) Range of measurement: 360° (in sixteen bearings).
Precision of measurement: ±11.25°.
Averaging time: 1 minute.

(B) Wind speed

(a) Wind speed is measured by the change of voltages generated in the AC

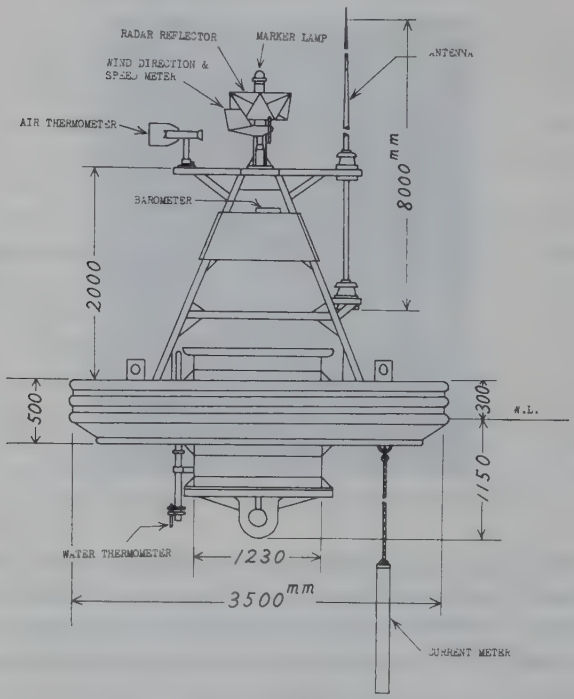

Fig. 2. Configuration of the No. 2 Buoy.

generator of a propeller type anemometer.

(b) The one minute average is provided by the electric circuit.

(c) Range of measurement: 2 m/sec~60 m/sec.
Precision of measurement: ±0.5 m/sec at the wind speed less than 10 m/sec, ±5% more than 10 m/sec.
Averaging time: 1 minute.

(C) Barometric pressure

(a) In the barometer, pressure change is transformed into the electric signal by attaching the hole generator to the bellows. We use a vacuum bellows as the pressure sensor and attach a temperature compensated bimetal to the tip of the bellows. The hole element tranduces the mechanical displacement

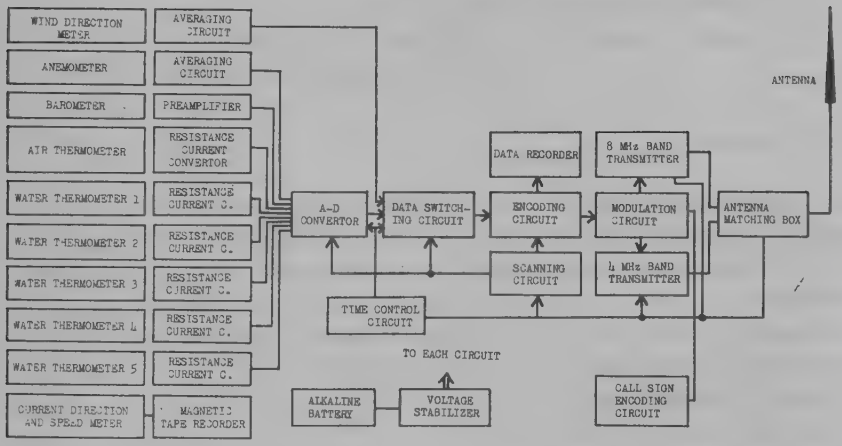

Fig. 3. The basic diagram of the No. 2 Buoy.

into an electric signal. The generator element, made of germanium (Ge), is located between the poles of a magnet.

(b) The barometer is inclosed in the outer case at the center of the tower, so that sea water spray and rain will not influence its operation.

(c) Range of measurement: 940 mb~1040 mb.
Precision of measurement: ±1 mb.

(D) Air temperature

(a) Air temperature is measured by transforming the temperature change to a voltage change by using Platinum-Thermoresistor and Wheet-Stone-Bridge-Circuit.

(b) The thermometer has been installed so that it will not be splashed with sea spray and rain.

(c) Range of measurement: −10°C~+40°C.
Temperature sensitive resistor: Platinum (Pt), 100 OHM (0°C).
Precision of measurement: ±0.5°C.

(E) Water temperature

(a) Platinum is used as the temperature sensitive resistor. In the present system the electrical cable has been inserted inside the steel core.

(b) Range of measurement: $-10°C \sim +40°C$.
Temperature sensitive resistor: Platinum (Pt), 100 OHM (0°C).
Precision of measurement: $\pm 0.5°C$ (for 1m, 10m, and 20m depth)
$\pm 0.2°C$ (for 30m and 50m depth).

3.2 Preamplifier

This circuit amplifies the small detection output from the bridge circuits of the air and water thermometers and provides an output into the A/D converter. It includes, internally, the linearizer to change the nonlinearity of the platinum temperature sensitive resistor to a linearized output signal. Output and input are independent of each other. The output is DC 10mA~50mA for $-10°C \sim +40°C$ in both cases. Rating and performance are as follows.

Output: DC 10 mA~50 mA
Input line impedance: Standard 1 OHM.
Precision: $\pm 0.5\%$ (full scale).
Power source: DC 24 V $\pm 10\%$.

3.3 Measurement system

(A) This is an automatic measurement method. This system measures and transmits automatically at the transmission time being one minute. Setting of the measurement time interval and transmission frequency is described in the following paragraphs.

(a) Measurements-transmissions may be timed for every hour, every three hours or every six hours, the actual period being preselected manually. These times include G.M.T. 00^h00^m, which is the standard.

(b) The transmission frequency is preselected to give either 4164.7 KHz, or 8330.2 KHz, or automatic alternative use.
(In the last case: $19^h00^m \sim 05^h00^m$, 4164.7 KHz
$06^h00^m \sim 18^h00^m$, 8330.2 KHz).

(B) A/D Converter

This device transforms the amplified analogue output of air and water thermometers to digital values in binary coded decimal form with 3 digits.

Its output is 900~999 for $-10°C \sim -0.1°C$
0~400 for $0°C \sim +40°C$.

Rating and performance are as follows:

A/D conversion method: Alternative comparison method.

Analogue input: 10 mA～50 mA.

Digital output: Binary coded decimal 3 figures.

Conversion accuracy: 1 bit.

Conversion speed: Less than 1 ms.

(C) Data switching circuit

In this circuit the outputs of the A/D converter, integrating counter circuit and A/D converter for clock use are made by the scanning circuit, which furthermore transforms the parallel information into series information.

(D) Scanning circuit

This circuit switches the output of A/D converter and the A/D converter for clock use. In addition it transforms the parallel information into series information and generates the scanning signal. The scanning of the A/D converter is carried out by this circuit.

(E) Parity bit addition circuit

This circuit inserts the odd number parity bit into the outputs from the A/D converter, A/D converter for clock use and the integrating counter circuit.

The relation between binary coded decimal digits and parity bits are as follows.

Decimal Number	Binary coded decimal number (with parity bit)				
	8	4	2	1	P
0	0	0	0	0	1
1	0	0	0	1	0
2	0	0	1	0	0
3	0	0	1	1	1
4	0	1	0	0	0
5	0	1	0	1	1
6	0	1	1	0	1
7	0	1	1	1	0
8	1	0	0	0	0
9	1	0	0	1	1

(F) Encoding circuit

This circuit encodes into short and long pulse code the binary coded decimal number from the output of the data switching circuit. This transforms the output "0" to a short pulse (20 ms) and "1" to a long one (60 ms), and inserts a space of 20 ms between each bit. In addition, it inserts the startmark of 240 ms in the first

part of frame and the interitems mark of 120 ms between two items.

(Example)

The case such as the scanning output 9; 10011 is as follows.

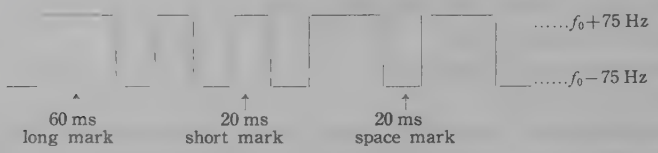

Here, f_0 is either the 4 MHz or 8 MHz band carrier.

(G) Clock control circuit

A crystal clock is employed as the basic reference. This circuit achieves an accuracy within a daily error of ±0.2 sec. The program timer is driven from this standard clock. The output is a one minute pulse. Contact points are closed at the set times by the rotation of a coder plate to give a variety of time outputs.

The time control circuit generates the following control output signals.

* Time information: 24 hours output, binary coded decimal 2 digits, 3 bits.

* A one minute pulse at every hour, or every 3 hours or every 6 hours, as preselected by manual operation.

* A ten minute pulse at ten minutes before the start of transmission. This time pulse is utilized to control the thermostat of the crystal oscillator.

* A four minutes pulse from three minutes before to one minute after transmission. This pulse is used for the control of A/D converter, preamplifier, wind direction unit, anemometer, barometer, and the air and water thermometers.

* Time information for the automatic switching of transmitter and antenna to select the suitable radio frequency for day and night.

3.4 Transmission system

(A) Modulation circuit

This circuit modulates the encoded signal to the F–S signal. In order to increase the frequency stability, temperature compensation and voltage stabilizing compensation techniques are employed. A frequency deviation of + 75 Hz for mark and − 75 Hz for space is used.

(B) Transmitter

This is a short wave band transmitter for transmission of meteorological and

oceanographic data. It uses one frequency in the 4 MHz band or 8 MHz band, and utilizes silicon transistors and a highly stabilized crystal oscillator.

Rating and performance are as follows.

Frequency: 300 Hz band width signal in the
4162.5～4166.0 KHz channel or the
8328.0～8331.5 KHz channel.

Output: 25 Watts.

Modulation type: F_1

Output impedance: 50 OHM.

S/N: Less than 40 dB.

Spurious radiation intensity: Less than 40 dB.

Transmission speed: 50 bauds.

Shifting frequency and deviation: 75 Hz, ± 10 Hz.

Frequency stability: 3×10^{-7}.

3.5 Antenna of buoy station

(A) A whip antenna of 8m length with a feeder of about 80 cm is used. The 8 m whip antenna is physically divided into four elements of about 1.5 m and a base element of about 1.2 m.

(B) Antenna matching box and switch.

This is for switching the antenna matching box to the suitable frequency for day and night. The switching signal comes from the clock control system.

3.6 Power source

A closed type of Ni-Cd cells used in this system. This Ni-Cd battery has merits in respect of temperature, maintenance, electric characteristic and so on, and is considered the most suitable for such kind buoy.

Capacity: 240 AH.

Output voltage: 1.2 Volt/cell.

Weight: about 12 kg/cell.

Number of cells used: 20 cells.

3.7 Voltage stabilizing circuit

This is the stabilizing circuit that divides the 24 volts of the battery into circuit

and sensor voltages and stabilises the voltage of each circuit.

Output voltage: 12V, 9V, 3V.

Stability: Less than ± 0.1 V.

3.8 Circuit for call sign

This circuit generates the call sign, JM2B, of the buoy station in Morse Code at the start of each transmission. This call sign is transmitted in A_1 modulation using a solid state Morse Code generator and a solid state transmitter power switch.

3.9 Data recording unit

This records the transmitted data. It is mainly intended to cover periods when the shore station is unable to receive signals because of bad ionospheric conditions. The method used is to transform the data sending signal (long and short pulse) into pulse of audio frequency and to record these on the magnetic tape. Sufficient recording capacity is available for 360 transmissions.

4. Shore station

The shore station is shown in Fig. 4 and its basic diagram is shown in Fig. 5. The shore station receives the data from buoy. The shore station consists of the reception system, the decoding system, the tape perforator, the data-writer, the electric power system, the control system and antenna.

4.1 Function of antenna

(A) Antenna

The antenna is parallel two wire system dipole functioning in both frequencies of 4 MHz and 8 MHz. It has the total length of about 36 m.

(B) Matching box

This is constructed by relays to match the 4 MHz or 8 MHz band radio receiver to the antenna, the relay being operated by the output of the time control circuit.

(C) Antenna switch

The function of this switch is to switch the 4 MHz band receiver and the 8 MHz band receiver, the relay being operated by the output of the time control circuit.

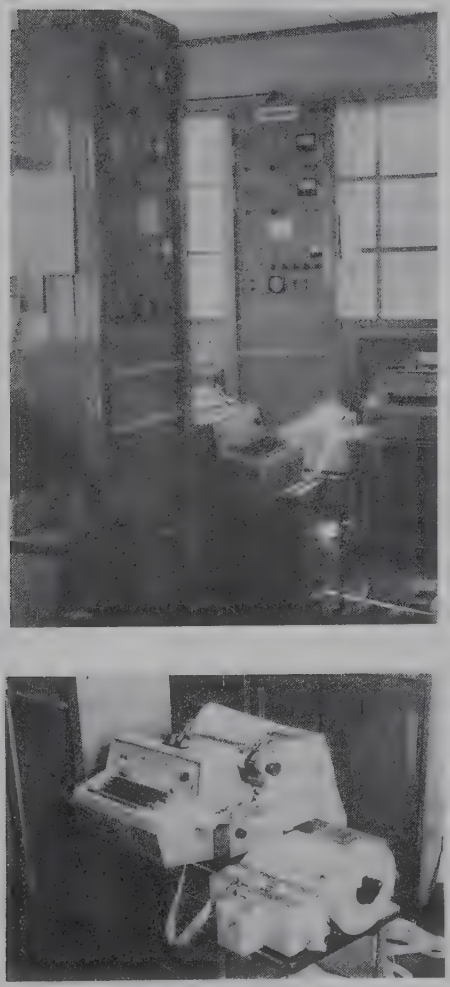

Fig. 4. The shore station at the Maizuru Marine Observatory.
Upper: Receiving equipment.
Lower: Perforator and data-writer.

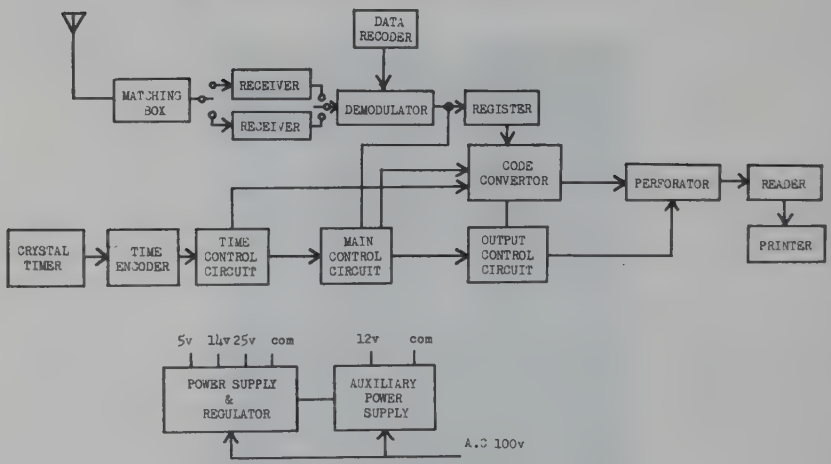

Fig. 5. The basic diagram of the shore station.

4.2 Receivers

(A) The reception section is composed of a 4 MHz band and a separate 8 MHz band receiver. In one set of the receiver, a 4 MHz band and 8 MHz band channel is included. It is of the rackmount type.

(B) Each receiver can be used for any one frequency in the 4 MHz band, 8 MHz and alternative usage by the external signal.

(C) Performance of 4 MHz and 8 MHz band receiver is as follows.

(1) Received frequency: SPOT reception of two frequencies such as 4162.5～4166.0 KHz and 8328.0～8331.5 KHz is possible.

(2) Wave type: F_1, F_2.

(3) Receiving method: Triple conversion super-heterodyne method.

(4) Intermediate frequency: First 1.85 MHz
Second 455 KHz
Third 2.975 KHz.

(5) Frequency stability: Less than 3×10^{-7} in 30 minutes from 5 minutes after power is applied.

(6) Input impedance: 50 OHM.

(7) Sensitivity: Less than 5μv, S/N: 20 dB.

(8) Image frequency selectivity: More than 40 dB.

(9) Selectivity: The selectivity of intermediate frequency circuit is variable.
In narrow at 100 Hz.
In wide at 425 Hz.

(10) Intermediate frequency output: More than 0.1 V at the load of 75 OHM. Here, antenna input is 5 μV.

(11) Variation of power voltage: No adjustments is necessary if the receiver voltage is within $\pm 5\%$ of the nominal supply voltage.

4.3 Reception and demodulation of signal system

(A) Clock control circuit

This comprises the programing timer, logic circuit and the standard clock. The standard clock is the crystal one that has a maximum mean daily error of ± 0.2 second and mean monthly error within 3 seconds. Its output is an 0.5 second contact signal every minute using vacuum enveloped contacts.

Rotation of the coder plate (time program) by the standard clock closes the contacts at the prescribed times and generates the time pulses.

This time control circuit generates control output signals as follows.

(1) Time information: In 24 hour-60 minutes system binary coded decimal 4 digits 16 bits.

(2) A 12 minutes pulse from 10 minutes before every hour or before every three hours or every six hours. This 12 minutes pulse is arbitrarily selective by manual operation and is used in the operation of the receiving system.

(3) A seven minutes pulse from one minutes before the scheduled start data reception. This is used to switch on the perforator and data-writer.

(B) Demodulation section

This is the circuit that demodulates the F–S signal from the receiver into pulse code. Received series information is transformed into parallel information, and memorized and registered by this circuit. A code check of received data is also carried out by this circuit. Output is generated only when data is validated by the code check.

4.4 Data transformation section

This section transforms the received data to five quantities such as wind direc-

tion, wind speed, barometric pressure, air temperature and water temperature at five depths. The output of this transformation section is displayed numerically in the display section.

4.5 Control circuit of perforator and data-writer

This circuit perforates received data on the perforator tape and drives the type-writer for tabulating and printing. This circuit generates also the control signal for tabulating and printing by data-writer and reading out automatically from the perforated tape after data reception has been completed.

4.6 Performance of perforator and data-writer

(a) Perforator
Code units: 8 units.
Perforation speed: 1200 letters/minute.
Input signal: 17 ms～20 ms.
Power: AC 100 V, 50/60 Hz.

(b) Data-writer
Standard type number: 95 letters/column.
Operation speed: about 500 letters/minute in standard.
Power: AC 100 V, 50/60 Hz.

(c) Type item
Observing day elapsed: Decimal number two column type.
Reception start time: 24 hour method, 4 digital letter type.
Observation time: 24 hour method, 4 digital letter type.
Observed value: Decimal number three column type in the specified column on every observation time.
Special information: Type the mark * in the specified column for each items.

4.7 Power supply section

Input voltage: AC 100 V within 10%, 60/50 Hz.
Out put voltage and current: DC 4～6 V 4A
DC 14 V 1A
DC 25 V 3A

DC 50 V 5A.

The power supply section is composed of the rectifier circuit, a "No Break" power circuit and the voltage stabilizing circuit. The rectifier circuit provides the equipment power from the service power. The voltage stabilizing circuit holds the circuit voltages constant. The "No Break" power source is used to power the time control circuit and consists of a "floating" alkaline battery. It has sufficient capacity for a continuous service power interruption for 72 hours.

5. Program cycle (at reporting times)

The time schedule is as follows.

$-10^m\,00^s$	Buoy station:	Crystal thermostat power "ON".
	Shore station:	Receiver power "ON" and stand by.
		Data reception and converter power "ON" and stand by.
$-3^m\,00^s$	Buoy station:	Analogue, digital converter, and all sensors power "ON" and stand by.
$-2^m\,00^s$	Shore station:	Data-writer and perforator power "ON" and stand by.
$-1^m\,00^s$	Buoy station:	Measurements of wind direction and wind speed begin to start (one minute averaged).
$-0^m\,00^s$	Buoy station:	Transmitter power "ON", sending of data.
	Shore station:	Reception of data, perforation of data starts.
$+1^m\,00^s$	Buoy station:	Transmission of data "STOP", data recording "STOP". Transmission power "OFF". All sensors power "OFF".
$+2^m\,00^s$	Shore station:	Tabulation, and print of received data.
$+6^m\,00^s$	Shore station:	Receiver, data-writer, tranduce circuit and data reception power "OFF".

6. Buoy construction

This buoy was constructed by the Buoy Division Office, Zeniya Aluminum Engineering LTD., Osaka, under the direction of J.M.A.

6.1 This buoy is composed of the following basic items.

(A) Float. (B) Tower for mounting sensors. (C) Case for housing the power

source and electronics equipment. (D) Marker lamp and radar reflector. (E) Buoy stabilizing weight.

6.2 Details

(A) Float

(a) The outer plate is made of an anticorrosive aluminum alloy plate.

(b) Polyurethane-foam is used internally (specific weight 0.04, total weight about 220 kg).

(c) The bottom of the float is fabricated from an integral circular plate to which is attached internal beam plates and the sides.

(d) Polyethylene pipes are attached to the perifloat for protection purposes.

(e) Metal fittings are attached to supports the current meter from the bottom of the buoy.

(f) A conduct pipe for the water thermometer cable is provided.

(B) Tower for mounting sensors

The tower is a four legged structure and is made of anticorrosive aluminum angle. The anemometer, air thermometer, barometer, connecting box, antenna, marker lamp, radar reflector, arm and base are attached at specified positions.

(C) Case for housing the power source and measurement equipment (internally).

(a) This case is made of anticorrosive aluminum alloy of adequate strength, and has an effective content volume of 1200×1300 mm and content weight capacity of about 400 kg. (b) Upper and lower float flanges are provided externally. (c) A base plate for weight fitting case is welded to the lower part. (d) The lid of the case has a radius of more than 600 mm and is water proof sealed by eyenuts and is also attached to the buoy by chain to prevent accidental loss in the sea. (e) Sensor's cables and a nitrogen gas valve are attached to the upper part of case. (f) The lower part of case is especially designed to prevent electrolytic corrosion. (g) A thermal barrier is attached to the lower surface of the lid. Canvas or similar covering is fitted to the upper part of the case.

(D) Marker lamp and radar reflector

(a) A Xenon lamp, that flashes every 2～3 second, used as the marker lamp and has a sun valve. A separate power supply is located in a thin cylinder attached to the lower part of the tower and has capacity for three months of lamp operation. (b) The radar reflector is made of aluminum alloy plate and

and is of the trigonal-pyramid type.

(E) Buoy stabilizing weight

This is fabricated from high quality coated iron and weights about 500 kg.

7. Meteorological and oceanographic data obtained from the buoys

Fig. 6 shows the positions of the buoy stations. The reception success rates for the No. 1 and No. 2 buoys accomplished at the Maizuru Marine Observatory are approximately 92 and 78 percent, respectively.

The 8 MHz frequency band was responsible for most of the success over that 500 km path. The 4 MHz frequency band was not so good owing to local electrical interference noise. Fig. 7 shows the general arrangement of the buoy and its mooring on this station. At Kiyose Communication Station, the signal strength of 8 MHz frequency band from the No. 2 buoy was always 30~50 dB, as shown in Fig. 8.

The data obtained from the No. 2 buoy from May to June 1970 is shown in Fig. 9. For reference, the data from the No. 1 buoy during the same period is also shown in Fig. 10.

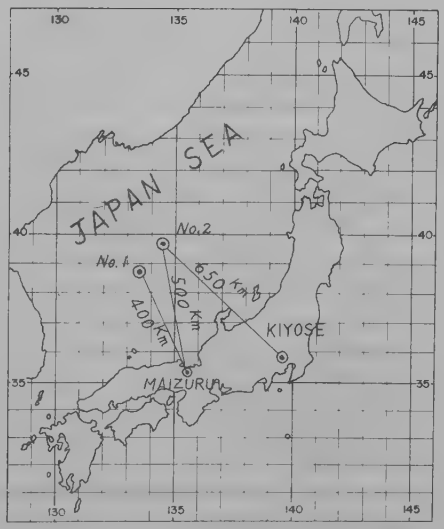

Fig. 6. The positions of Bouy Stations.

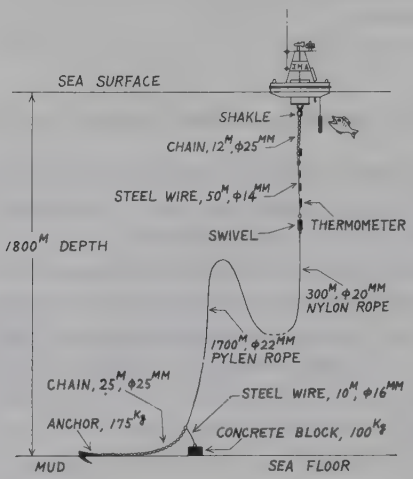

Fig. 7. Bouy and mooring configuration.

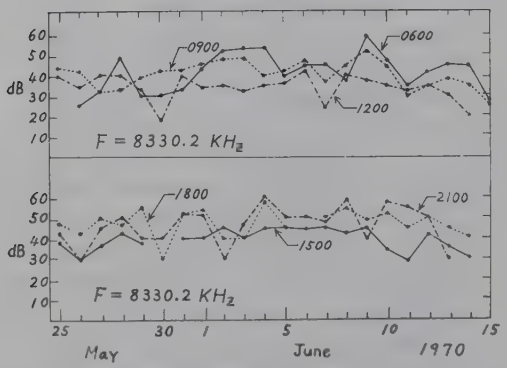

Fig. 8. The signal strength obtained from the No. 2 Bouy at the Kiyose Communication Station.

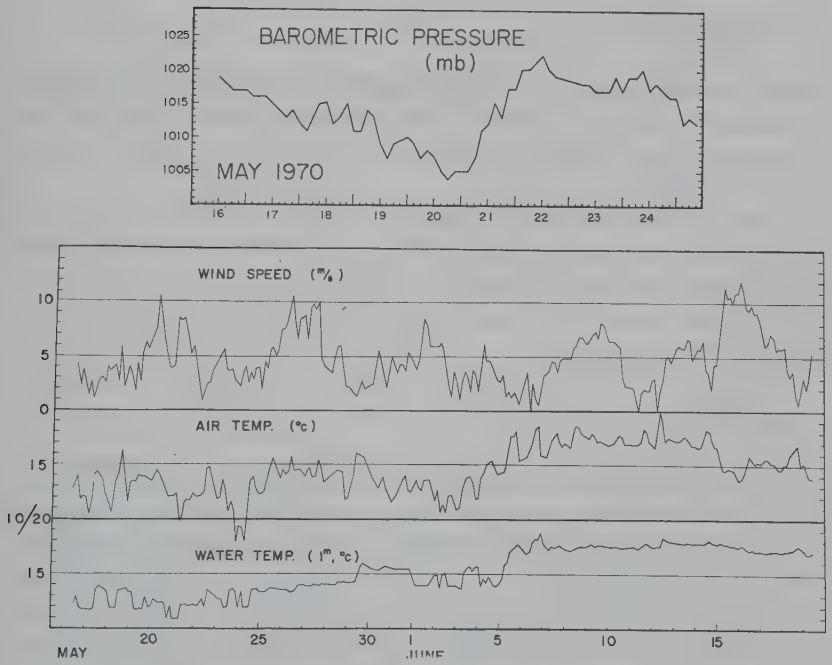

Fig. 9. Barometric pressure, wind speed, air temperature and water temperature obtained from the No. 2 Buoy (16 May to 19 June, 1970).

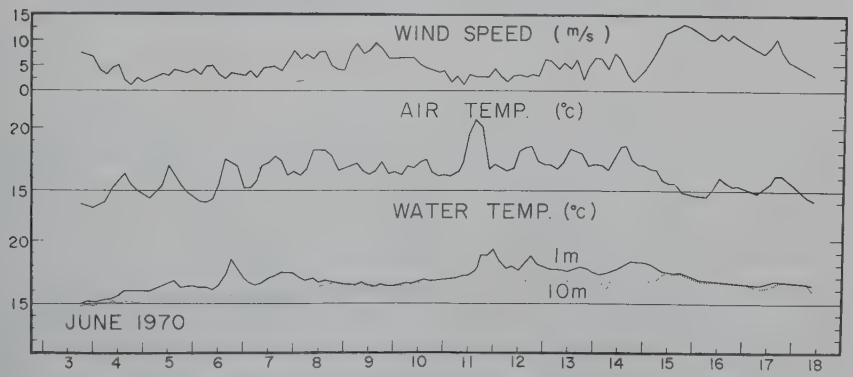

Fig. 10. Wind speed, air temperature, and water temperature obtained from the No. 1 Buoy (3–18 June, 1970).

8. Concluding remarks

Radio Telecommunication Division, Matsushita Communication Industry Co., LTD. is presently engaged in conducting the engineering evaluation test of these general-purpose buoys developed under contract for the J.M.A. and the Maizuru Marine Observatory.

The first operation of the No. 1 buoy at sea was carried out at the middle part of the Japan Sea between October and November 1969, and the No. 2 buoy was built incorporating the operational experience gained from the No. 1 buoy.

At the present stage of development some further improvement to the buoy antenna system is required.

Acknowledgements

The author wishes to express their thanks to all members of the officers and crew of the Ryofu-Maru for their cooperations throughout the operation of the buoy, and to Dr. I. IMAI, Director of Marine Division, J.M.A., all members of the Ocean Data Buoy Committee in J.M.A., Mr. M. KAGARI, Director of the Maizuru Marine Observatory, Mr. M. KATAYAMA, Chief of Radio Communication Section, Meteorological Communication Station at Kiyose, and to Mr. S. KATSUMATA, Radio Telecommunication Division, Matsushita Communication Industrial Co., LTD., for their kind helps. The author also indebted much to Mr. Ralph de la LANDE, Commonwealth Bureau of Meteorology, Melbourne, for his critical reading of the manuscript.

The Oceanographical Magazine
Vol. 22, No. 2, pp. 95 to 123, December 1970

Maritime meteorological summary of the western North Pacific Ocean in the winters of 1967, 1968 and 1969

Shigeaki HAYASHI, Hiroshi TAKANO and Asahi YAMASHITA

Japan Meteorological Agency

(Received August 17, 1970)

Abstract: A cruise for the Cooperative Study of the Kuroshio and Adjacent Regions (CSK) was made in each winter of 1967, 1968 and 1969 in the western North Pacific Ocean by the R.V. *Ryofu Maru* of the Japan Meteorological Agency. We made routine surface observation 8 times a day, weather radar observation twice a day, and sometimes special observations such as aerological observation and measurements of radiation from the sky and sea for the study of air-sea interraction. We tried to describe comparatively air temperature, dew point temperature along long. 137°E from Japan to New Guinea, since this course had a little differnce of time as compared with other courses. Our discussions were made about cold and dry subtropical anticyclones over the Asiatic continent, the Asiatic monsoon, and extratropical cyclones, and for the tropical regions about the northeasterly North Pacific trades, Indian Ocean monsoon and South Pacific trades. During the Northern Winter tropical cyclones rarely occur, and the Intertropical Convergence Zone sometimes invades the Northern Hemisphere.

Another study is concerned with the diurnal variation of upward and downward radiation and also with the latitudinal change of radiation balance through the sea surface in low latitude region.

1. Introduction

Maritime meteorological observations for the Cooperative Study of the Kuroshio and Adjacent Regions (CSK) were carried out in the winters of 1967, 1968 and 1969. Routine surface observations were carried out 8 times a day, namely: 00, 03, 06, 09, 12, 15, 18 and 21 GMT, and the data was transmitted to the Japan Meteorological Agency, Royal Observatory in Hong Kong, Manila Weather Bureau and Guam Weather Station. The cloud observation by the weather radar on board was carried out twice a day, at 00, 06 GMT. Under good weather conditions special observations of upward and downward radiation from the sky and sea were made by the pyrheliometer and pyrgeometer on the equatorial parts along long. 137°E in 1968 and 1969.

2. Wind systems

Figure 1 shows the northerly or northeasterly Asiatic monsoon, the northeasterly trades in the Northern Hemisphere, and the South Pacific trades or the South Indian Ocean monsoon along long. 137°E.

According to these data compared with the mean wind speed and the most frequent wind direction which are taken from the Pilot Chart (U.S. Navy, 1943), the most frequent wind is almost northeasterly with a mean speed of 15 knots in the subtropics and of about 5 knots or less in the tropics. The northwesterly wind, the Asiatic monsoon, extends from the southern coast of Japan to lat. 30°N in 1967, and as far south as lat. 25°N in 1968, because an extratropical cyclone on the Polar front moved to the northeast along the east side of Asiatic continent. In

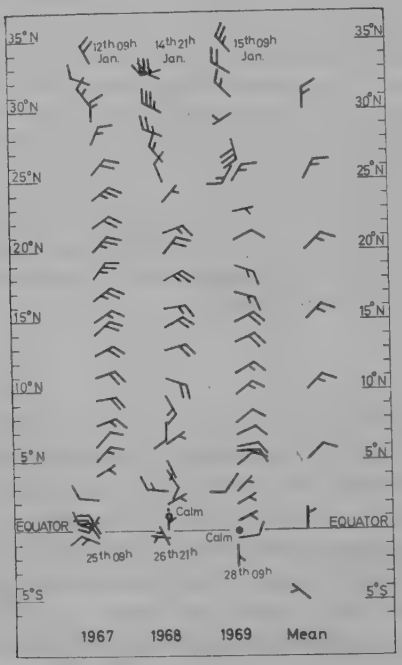

Fig. 1. The distribution of wind direction and wind speed along long. 137°E in January 1967, 1968 and 1969.

1969 the northwesterly wind flowed to the north of lat. 30°N and the wind direction and speed in the area from lat. 30°N to 25°N were not stable due to an extratropical cyclone which passed near lat. 25°N.

The North Pacific Trades were stronger in 1967 than in the other years. The wind in 1969 was weaker than the mean. The trade winds in the Equator Countercurrent region to the south of lat. 7°N are much influenced by the Philippine Islands and New Guinea. The South Pacific Trades and South Indian Monsoon were blowing alternately in the vicinity of the Equator, so there existed weak speed zone having unstable wind direction. In 1969 the wind speed was larger than in the other years and its direction was westerly or northwesterly at near the Equator.

3. Air temperature, dew point temperature and sea surface temperature

3.1 Air temperature

Let's examine the air temperature along long. 137°E for those three years (Fig. 2). The air temperature was lower in 1968 than in 1967 and 1969 because of the outbreak from the Asiatic anticyclone. The air temperature increased rapidly in the neighborhood of lat. 25°N in 1969, because an extratropical cyclone passed through from west to east along the parallel of lat. 25°N, and the northern branch of North Pacific Trades which was modified thoroughly by the absorption of heat and moisture from the sea surface flowed into above mentioned extratropical cyclone.

The air temperature in each year increases only slightly in the area from lat. 16°N to 7°N, the North Equatorial Current Zone, and the maximum air temperature is about 28°C. Over the Equatorial Countercurrent Zone from lat. 7°N to 2°N, it is obvious that the air temperature shows a similar tendency for those three years, and but fluctuates by the influence of the trades, ocean currents and precipitations. However, the air temperature shows a decreasing tendency in the area of the Equator, because of the topographical influence by New Guinea.

3.2 Dew point temperature

The dew point temperature along long. 137°E in each year is shown in Fig. 3. The dew point temperature south of Japan was lower in 1968 than in 1967 and 1969 because the predominant and dynamic anticyclone was over the Asiatic continent and the outbreak from this anticyclone extended probably to further the southern

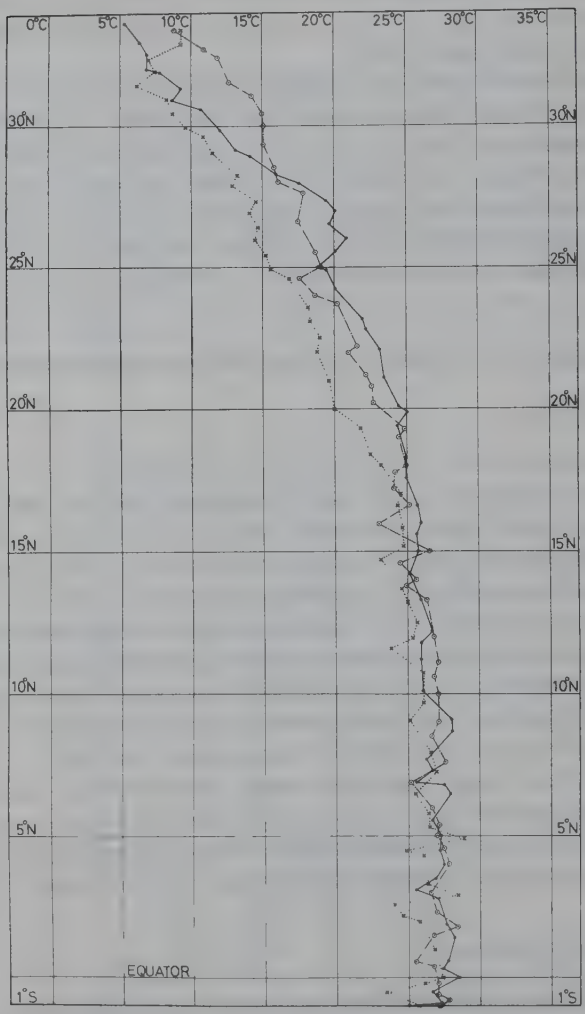

Fig. 2. The distribution of air temperature along long. 137°E in January 1967, 1968 and 1969. Dot-dash-line: air temperature in 1967. Dotted-line: air temperature in 1968. Solid-line: air temperature in 1969.

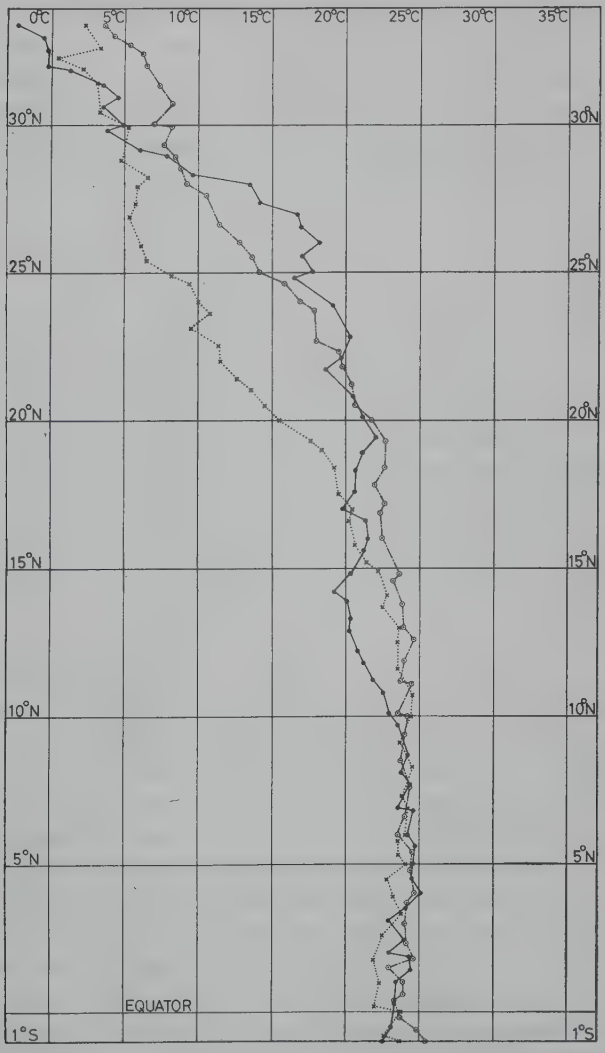

Fig. 3. The distribution of dew point temperature along long. 137°E in January 1967, 1968 and 1969. Dot-dash-line: dew point temperture in 1967. Dotted-line: dew point temperature in 1968. Solid-line: dew point temperature in 1969.

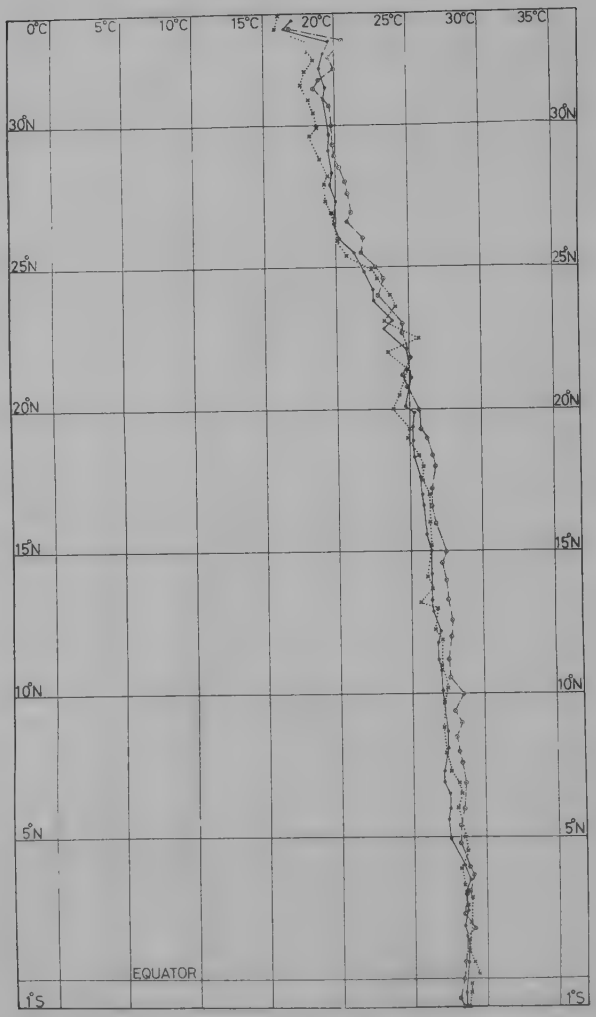

Fig. 4. The distribution of sea surface temperature along long. 137°E in January 1967, 1968 and 1969. Dot-dash-line: sea surface temprature in 1967. Dotted-line: sea surface temperature in 1968. Solid-line: sea surface temperature in 1969.

waters of Japan. The dew point temperature in 1969 increased rapidly at near lat. 27°N as well as the air temperature. Especially, the anticyclone spread from the Asistic continent to the southeast in the winter of 1969 and stayed in the area from the Philippines to the waters south of Japan. Thus, dew point temperature between about lat. 17°N and 10°N was lower than in 1967 and 1968. However, the change of dewpoint temperature over the Equatorial Countercurrent was not so large, because the maritime air mass of the central Pacific Ocean coverd the region.

3.3 Sea surface temperature

The sea surface temperature along long. 137°E (Fig. 4) increases rapidly in the vicinity of lat. 33°N in each year, where we find the north limit of the Kuroshio. The distribution of sea surface temperature is similar to those of air temperature and dew point temperature. Sea surface temperature increases southward gradually, though slightly in the North Equatorial Current, and usually was not more than 30°C. The sea surface temperature was higher in 1967 than in 1968 and 1969.

As described in the former report (HAYASHI, MIYASHITA and FUJITA, 1968), sea surface temperature reached 30°C near lat. 6°N and 3°N in 1967 probably due to the meteorological influence. However, these unusual high temperatures might not be certain.

4. General remarks

We made surface stream-line charts for 00 GMT every day in 1968 and 1969, and calculated pseudo-adiabatic wet-bulb potential temperature along long. 137°E in each year for the air mass analysis (Fig. 5). The analysis shows clearly that the Asiatic continental air mass spreads from the south coast of Japan to lat. 20°N, and degenerates rapidly due to the absorption of heat and moisture from the warmer sea surface. Pseudo-adiabatic wet-bulb potential temperature varies between about 5°C and 23°C over this meridional section, and increases gradually in the area from lat. 20°N to 5°N in the North Equatorial Current, particularly, there are not so large changes between lat. 9°N and 5°N.

Further to the south lat. 5°N, the variations of each year show clearly the existence of the flow which flowed out of tropical maritime air mass of both hemispheres. The variations of pseudo-adiabatic wet-bulb potential temperature lat. 30°N in 1967 changed gradually, because the cold front that streached from the extratropical

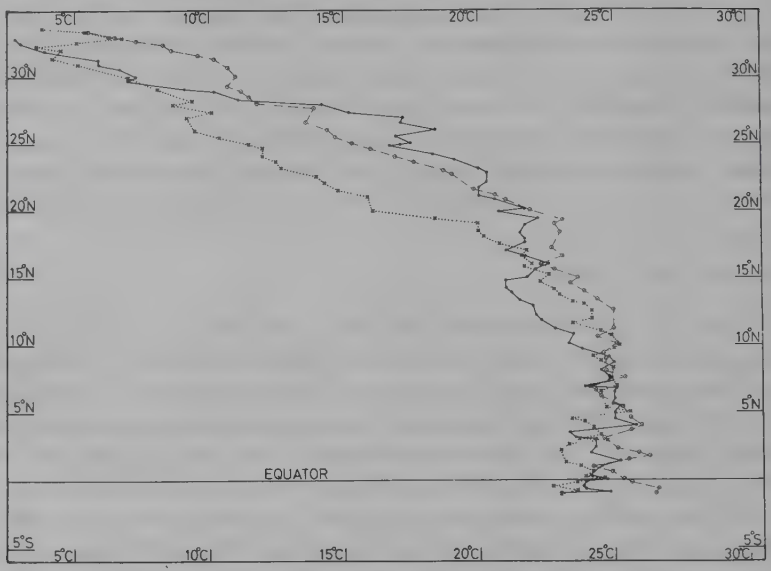

Fig. 5. The pseudo-adiabatic wet bulb potential temperature along long. 137°E in January 1967, 1968 and 1969. Dot-dash-line: 1967, Dotted-line: 1968, Solid-line: 1969.

cyclone in the southern waters of Japan passed through. The variations of pseudo-adiabatic wet-bulb potential temperature in the area between lat. 34°N and 30°N in 1968 clearly shows that a low pressure trough was passing and the Asiatic anticyclone extended to far southern waters of Japan.

4.1 January

The weather in January of 1967 was the same as that of the average year. The anticyclone over the Asiatic continent was strong at the beginning and middle of the month, and weak at the latter part. As a result, the northwesterly monsoon was stronger and the northeasterly wind predominated over the South China Sea. The Ogasawara maritime air mass existed in the central part of the North Pacific Ocean, and the North Pacific Ocean trades predominated very much in the central area of the North Pacific Ocean. Its average wind speed was about 20 knots. The weather in the northwesterly monsoon belts was changeable and cloudy with in-

termittent rain and scattered shower, but the weather in the northeasterly trades was fine.

The weather in 1968 was a little warmer than usual. There were four remarkable outbreaks of the Asiatic anticyclone. The maritime air mass remained in the southern part of the central Pacific Ocean and the northeasterly trades were predominant in the area from lat. 20°N to 10°N. In the tropical area, the weak tropical depression moved from east to west and the branch of the northwesterly monsoon and northeasterly trades flowed in the tropical depression. The average wind speed of the northeasterly trades was 18 knots.

The outbreak from the Asiatic continent air mass was stronger at the beginning of January in 1969 and after that it became weak in the south of Japan because the maritime air mass spread to far southern waters of Japan and the polar front became nearly stationary on the south coast of Japan. The trough of pressure existed often between the Philippines and the eastern part of the South China Sea, and the Philippines was covered with high pressure belt. Thus, northeasterly trades was more weakened in 1969 than in the other years. The averaged wind speed of the northeasterly trades was about 15 knots.

The tropical depression Phyllis occured at lat. 8°N, long 167°E on January 17, 1969, and she moved to the west. A detailed discussion about this tropical depression will be made in future. The weather situation in the surface and upper air on January 18, 1969 is shown in Fig. 6 and 7. On the 700 mb surface (Fig. 7) the Westerlies dominated over the north area of lat. 25°N, and extended over the northwesterly monsoon or the northeasterly trades at the surface. The Thailand, the northeastern part of the Philippines and the area of lat. 20°N, long. 155°E were covered with subtropical anticyclones. These anticyclones formed the subtropical high pressure belt between lat. 10°N and 30°N. The northeasterly trades from the southern part of the subtropical high pressure blet streamed into the southern part of the South China Sea up to the Equator. On the other hand, a branch of the northeasterly trades streamed into the weak tropical depression north of New Guinea.

The surface situation on January 18, 1969 is shown in Fig. 6. The anticyclone (1,033 mb) centerd at lat. 33°N, long. 133°E moved eastward at a speed of 15 knots. The anticyclone (1,020 mb) was stationarily located on the China Mainland. The anticyclone (1,024 mb) located at lat. 30°N, long. 160°E was moving eastward at a speed of 12 knots. The extratropical cyclone (1,018 mb) existed in the East China Sea and the extratropical cyclone (1,016 mb) centered at lat. 31°N, long. 148°E was

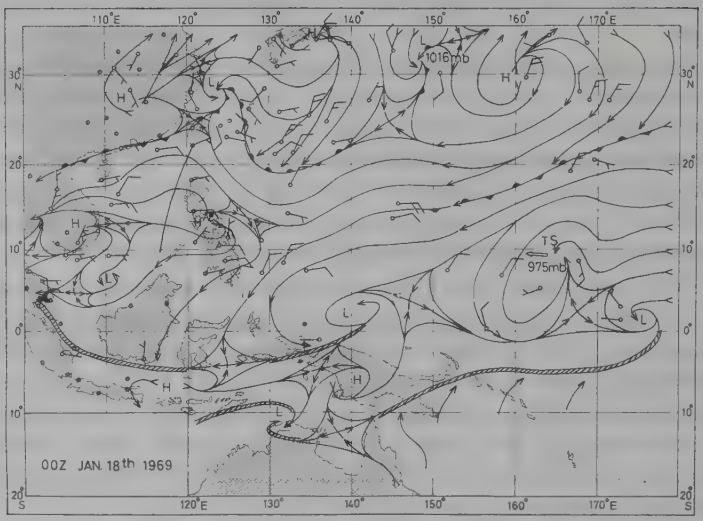

Fig. 6. Stream line at surface. 00Z. January 18, 1969.

moving eastward at a speed of 30 knots. The front stretches from this cyclone to the south of Japan, and the stationary front lay at full length east and west in the south coast of China Mainland. The noticeable wavy trough of pressure existed in the South China Sea. The polar front extended to the east of the Philippines and reached the weak tropical depression to the north of New Guinea. The tropical depression Phyllis (975 mb) at lat. 9°N, long. 166°E, and moving westward became a typhoon. The wind was strong in the northeast section of this typhoon.

The northeasterly monsoon extended to the Philippines, and a northern branch of the northeasterly trades became to the southeasterly wind in the east of the Philippines, which was prevailing in the northern area of the South China Sea and in the southern part of China Mainland. Thus, the above-mentioned stationary front was caused by the southeasterly wind and the northeasterly monsoon from Asiatic continent. The southern branch of the northeasterly trades extended to the southeast of Philippines and to the northeast of New Guinea. These trade-winds crossed the Equator and invaded the Banda Sea.

The north limit of Intertropical Convergence Zone existed to the north of Australia and the high pressure belt in the Northern Hemisphere extended southward.

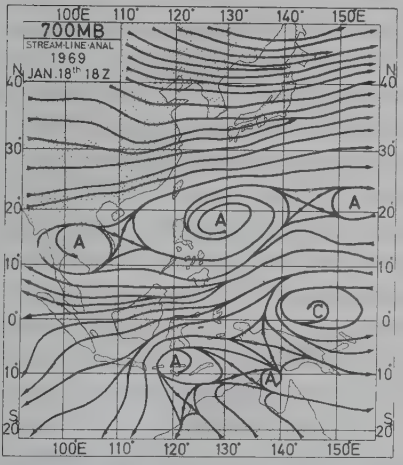

Fig. 7. Stream line at altitude 700 mb surface. 18Z. January 18, 1969.

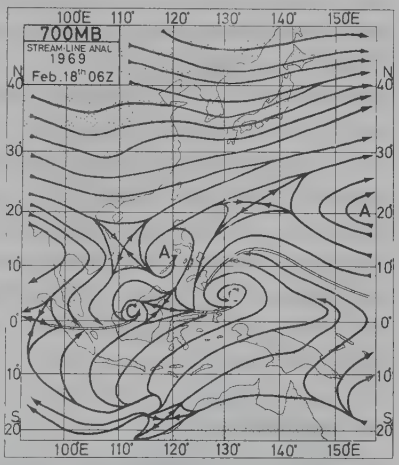

Fig. 8. Stream line at altitude 700 mb surface. 06Z. Feburary 18, 1969.

The neutral corner of convergence or divergence was located east of the Philippines, and the wind direction and the wind speed there was unstable and weak, and shower was scattered all over. As shown above, the important weather element is the outbreak of the monsoon, extratropical cyclone with a front and the trades. The wavy through of pressure exists frequently over the South China Sea.

Commonly, the Intertropical Convergence Zone exists in the Southern Hemisphere, and its north limit rarely invades the Northern Hemisphere. The tropical depression or the typhoon occured more rarely in 1969 than in the other years.

4.2 February

The maritime air mass was further west in February than in January for 1969. The subtropical anticyclone over the Asiatic continet was stronger than the former month, and the frontal zone was formed south of Japan.

The stream lines on the 700 mb surface on February 18, 1969 are shown in Fig. 8. The Westerlies were as far south at lat. 30°N, and the center of anticyclone was located at lat. 20°N, long. 150°E. Another anticyclone extended over the Philippines. The diverging air was flowing into a tropical cyclone in the

Celebes Sea of the Southern Hemisphere. There was a weak tropical cyclone in north Borneo Island. On the other hand, the northern branch of the diverging air flowed east along the north side of subtropical anticyclone, and then northeastward. The Intertropical Convergence Line between these tropical cyclones invaded near lat. 10°N. The wavy trough of pressure extended to the South China Sea.

On the chart of surface stream-line on February 18, 1969 (Fig. 9) we find an anticyclone (1,046 mb) on the Asiatic continent, an anticyclone (1,025 mb) in the North Pacific Ocean and an anticyclone (1,020 mb) south of Japan. Extratropical cyclones near Okinawa and south of Japan were moving to the east. The stationary front in the southern parts of China continent lengthened in the east—west direction. The northwesterly and northeasterly monsoon was weak, but the northeasterly trades was stronger than the monsoon. The wind direction in the South China Sea was mainly east and the wind speed was weak because of the above mentioned stationary front.

There was the equatorial low pressure belt over the Equatorial Countercurrent and the equatorial high pressure belt in the Southern Hemisphere. Thus, the Intertropical Convergence Zone invaded the Northern Hemisphere. The most important

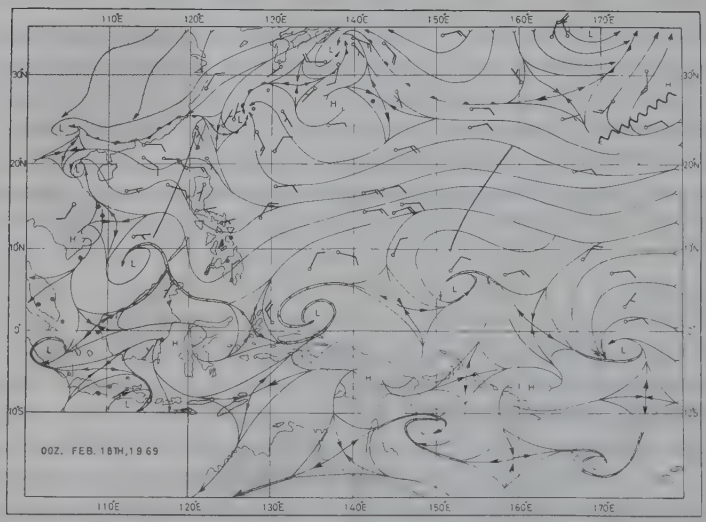

Fig. 9. Stream line at surface. 00Z. February 18, 1969.

weather element in this month was the extratropical front between the southeast coast of Asia and north of the Philippines. The trough of pressure extendes to the east side of the South China Sea. The typical weather in the north side of the extratropical front was overcast with Stratocumulus, Stratus fractus. It rained on and off. The wind direction was north or northeast. On the other hand, the weather in the south side of this front was fine or cloudy with some Cumulus, and the wind direction was easterly or northeasterly. In the South China Sea, generally, the wind direction was northeasterly, and the wind speed was greater in February than in other months. Sometimes, however, the wind direction veers east and its speed becomes weak, it seems that the stationary front extends to near the Asiatic coast.

4.3 March

The stream line on the 700 mb surface on March 11, 1969 (Fig. 10) shows that the Westerlies predominated over north Japan, and the subtropical anticyclone was laying over the western North Pacific Ocean and the South China Sea. The northeasterly trades reached near the Equator, and a branch of this flow was connected to a weak tropical depression near lat. 8°N, long. 154°E.

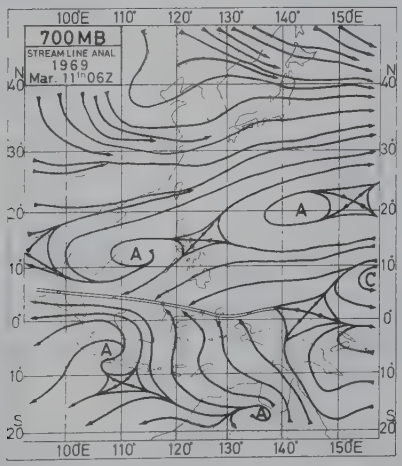

Fig. 10. Stream line at altitude 700 mb surface. 06Z March 11, 1969.

In the Southern Hemisphere, an anticyclone existed over Indonesia and Australia. Both southeasterly monsoon and the southwesterly trades or the South Pacific trades blew toward the Equator. The Intertropical Convergence Zone invaded north of the Equator.

The stream line at the surface on March 11, 1969 is shown in Fig. 11. The extratropical cyclone (1,020 mb) at lat. 31°N, long. 143°E was moving eastward at a speed of 20 knots. The other extratropical cyclone which (1,020 mb) was located in the south area of the East China Sea. As a result, both cold and warm front were fastend between these extratropical cyclones. The radar's echos of remarkable cold front are shown in Fig. 12, 13, 14, 15, 16 and 17 for reference. A subtropical anticyclone was located lat. 22°N, long. 145°E east of the Philippines. A weak tropical depression occurred near lat. 2°N, long. 155°E. The wind speed in the northeast area of this depression was greater than in the other area. The trough of pressure extended between the East China Sea and the South China Sea. The northeasterly monsoon from the Asiatic continent was weak. The northern branch of northeasterly trades became the southeasterly wind east of the Philippines and was flowing in the extratropical cyclone in the East China Sea. On the other

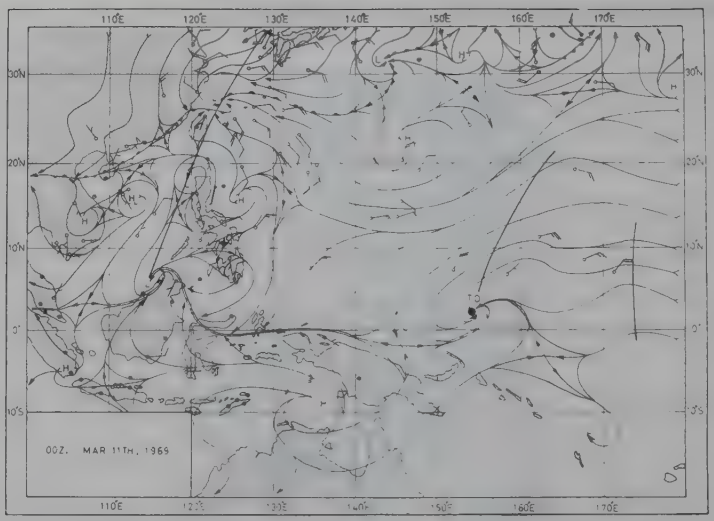

Fig. 11. Stream line at surface. 00Z. March 11, 1969.

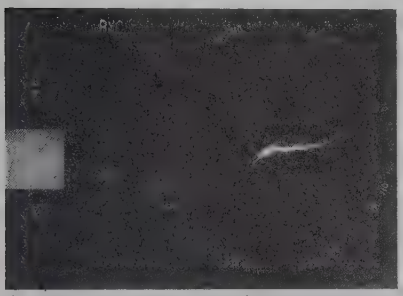

Fig. 12. The PPI echo picture shows the passage of cold front. 00Z. March 12, 1969. The position is lat. 16°59′N, long. 123°52′E.

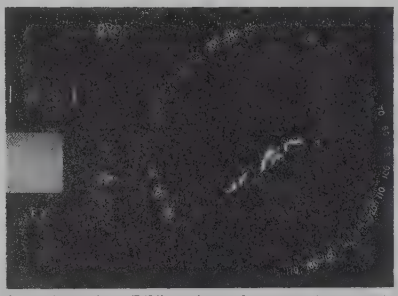

Fig. 15. The PPI echo picture shows the passage of cold front. 05Z. March 12, 1969.

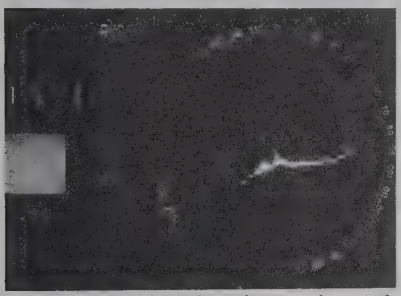

Fig. 13. The PPI echo picture shows the condition of Figure 12 after an hour.

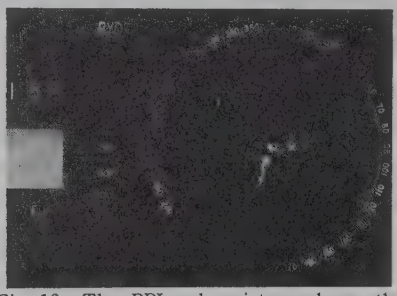

Fig. 16. The PPI echo picture shows the passage of cold front. 06Z. March 12, 1969. The position of ship was lat. 17°N, long. 124°22′E. The northern echo may be looked as instability line.

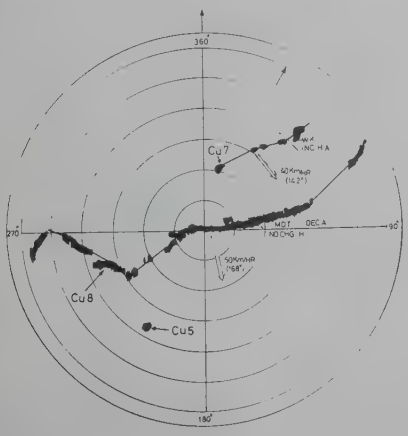

Fig. 14. The analysis of PPI echo. 00Z. March 12, 1969. Reference to Figure 13.

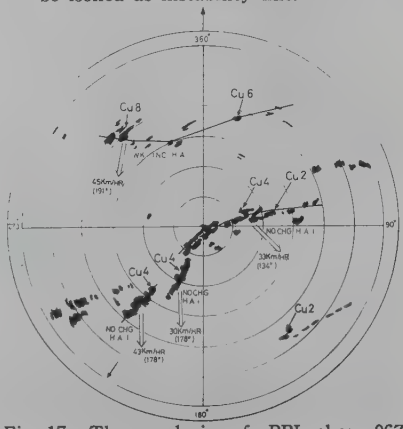

Fig. 17. The analysis of PPI ehco. 06Z. March 12, 1969.

hand, a southern branch of the northeasterly trades reached the vicinity of the Equator. The northeasterly trades converged with the South Indian monsoon and the South Pacific trades. The Intertropical Convergence Line was located between the above-mentiond tropical depression and a weak tropical cyclone north of Borneo Island. An equatorial low pressure belt extended near the Equator.

5. The monsoon and the trades

Here we describe roughly about the monsoon and trades. On the south area of the Asiatic continent the monsoon blows as a northwesterly or northeasterly wind, and the relatively cold and dry air is transformed into the warm and wet air over the warm Kuroshio (Fig. 2, 3 and 5), and so there is a very rapid transformation of the air mass. When the air is warm at the sea surface, lapse rate is steepened, and the momentum of the air may increase along the vertical. Also, the extratropical cyclone passes frequently through the region. The distribution of subtropical anticyclone in winter is shown in Fig. 18. The anticyclone with uniform temperature is always situated in the subtropical region. On the east side of such a sub-

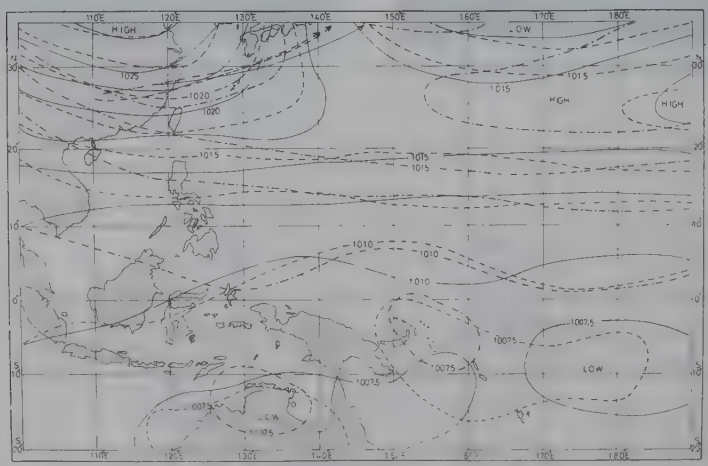

Fig. 18. The distribution of average isobaric line in January, February and March, and the average track of extratropical cyclone. Solid line: average isobaric line in January. Broken line: average isobaric line in February. Dot-dash-line: average isobaric line in March.

tropical anticyclone, there is persistently subsiding motion. The moisture absorbed from the ocean is limited to the surface layer, and above this the relative humidity is very low, generally, of the order 20 to 30 per cent (PETTERSSEN, 1958). However, there is generally a little ascending motion in the west area of this anticyclone. We analysed the moisture at the surface in the west and east area of the subtropical anticyclone. Dew point temperature at Guam Island (lat. 13°29′N, long. 144°48′E) was 22°C on January 17, 1969 and 20°C at Wake Island (lat. 19°17′N, long. 166°39′E) on January 26, 1969; the former was 20°C and the latter was 18°C; on Feburay 10, 1969 the former was 20°C and the latter was 17°C. Both Guam Island and Wake Island are situated in the northern part of North Equatorial Current.

The vertical cross section along long. 140°E on January 27, 1969 (Fig. 19) shows that evaporation from the sea surface was more in the subtropical area than in the tropical area. On the equatorial side of the subtropical anticyclone, the flow from the anticyclone met the South Indian trades or the South Pacific trades in the vicinity of the Equator.

There is general ascending motion in the Convergence Zone. It seems that

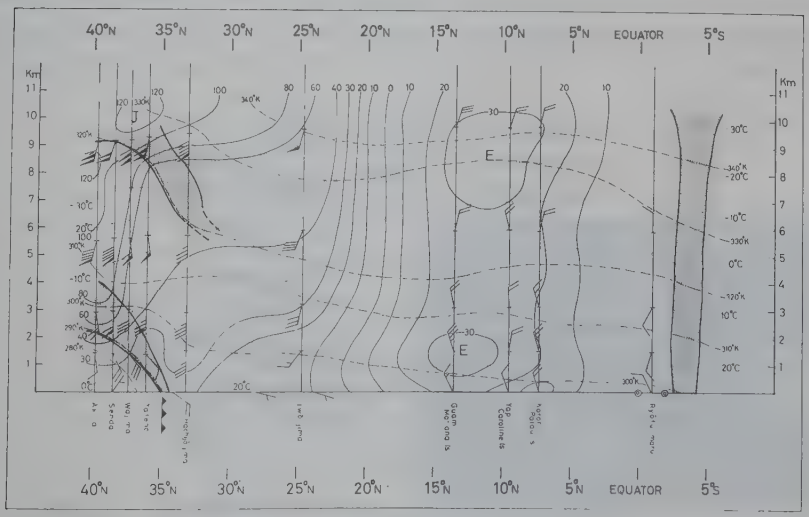

Fig. 19. Vertical cross section along long. 140°E on January 27, 1969. Solid line: wind speed in knots, Dotted-line: air temperature in °C. Dot-dash-line: equivalent potential temperature in°K.

the lapse rate is steep, and the condition of heat and moisture up to high levels is lively (PETTERSSEN, 1958). The Convergence Zone often is not a simple line but has a complex character (RIEHL, 1954). The monsoon streams as the northeast wind over the South China Sea, though in the vicinity of Japan, north or northwesterly. The northeasterly monsoon in the South China Sea is generally accompanied by dry fair weather. The wind is usually steady, its speed being about 28 knots or more. According to our observation the average speed of the trades in the Northern Hemisphere was from 15 knots to 20 knots (Fig. 1), and these trades in the Southern Hemisphere streamed as a northwesterly wind over the South Indian Ocean as far south as lat. 10°S, the Arafra Sea, and the northern Australia. The wind in the equatorial low pressure belt was weak and unstable. The semidiurnal pressure oscillation was regular, the maximum about 10 A.M. and 4 P.M., the minimum about 4 A.M. and 10 P.M.

On the echo of weather radar on January 28, 1969 (Fig. 20 and 21) at lat. 0°57′S, long. 137°01′E, there are many Cumulus congestus and Cumulonimbus capillatus with showers and some Stratiform clouds. The top of these clouds were from 6,000 m to 11,000 m high. The ceiling of Cumulus fractus was about 500 m. The intensity of echo was moderate, because showers were not so heavy. The increase and decrease of echo's intensity, areas, and vertical motion did not appear within an hour.

Fig. 20. The radar echo of clouds which developed along vertical in the vicinity of the Equator. The position is lat. 0°57′S, long. 137°01′E (00Z, January 28, 1969).

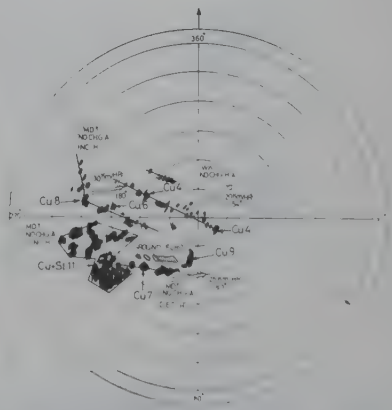

Fig. 21. The analysis of PPI echo picture in Figure 20.

6. The Intertropical Convergence Zone

The trade-winds of both hemisphere converge in the equatorial low pressure belt "Doldrums". The zone of converging wind is 100 to 200 km "Intertropical Convergence Zone (ITC)". During winter in the Northern Hemisphere, generally, ITC moves southward as far south as lat. 10°S. According to our study, the north limit of ITC sometimes invaded a zone of the Equatorial Countercurrent.

Let us consider the stream line charts at the 700mb surface on January 29, 1969 (Fig. 22). The north limit of ITC lay on the tropical area in the Northern Hemisphere, and the south limit existed along lat. 10°S and westward long. 120°E. A tropical cyclone existed around lat. 4°N, long. 154°E. Next, we describe about the condition of sea surface (Fig. 23). In the area of low latitude, a tropical cyclone existed on the north Borneo, and another tropcial cyclone (1,004 mb) existed near Tarawa Island (lat. 1°21′N, long. 172°55′E). The wavy trough of pressure extended to the South China Sea and the easterly wave lay in the Pacific Ocean.

The north limit of the ITC lay along the Equator, and the south limit extended along lat. 10°S. However, it seems that the ITC became a line at the east of New Guinea and moved eastward, because the tropical low pressure belt extended to this region. What is evident in comparing the conditions of the surface and the upper is that the north limit of the upper invaded the north side area of the

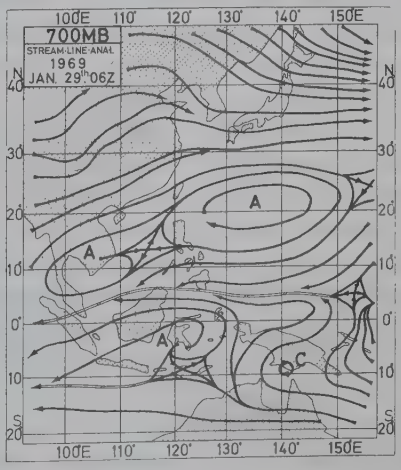

Fig. 22. Stream-line at altitude 700 mb surface. 06Z. January 29, 1969.

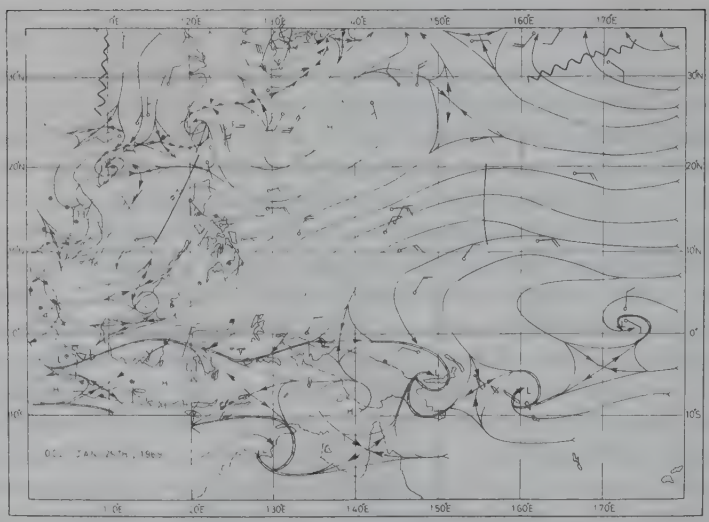

Fig. 23. Stream line at the surface. 00Z. January 29, 1969.

Equator but the north limit of the surface extended to the south side of the Equator. The charts of stream line at the 700 mb surface, and at sea surface, and of radar's echo on January 31, 1969 are shown in Fig. 24, 25, 26 and 27.

The radar's echo at lat. 3°N, long 133°24′E shows that neutral corner with ITC extended to the southwest of our ship. All clouds were moving southwest in the northeasterly trades. There were many Cumulonimbus capillatus with showers. A large group of Cumulonimbus with showers extended widely southward as far as 100 miles away, and clouds lines up nearly at regular intervals. The level of echo cloud's top was from about 3,000 m to 6,000 m. These clouds were moving at a speed of about 20 km/hr, and the southern group moved more slowly than northern ones. We observed that the wind direction was northeast and the speed was 15 knots, and the cloud's types were Cumulonimbus capillatus, Cumulus congestus, Altocumulus stratiformis translusidus and Altostratus opcaus. The ceiling of Cumulus fractus was 300 m. The stracture of Fig. 20 and 21 may show the condition of nearly north limit of ITC.

If we pass southward through ITC, we may observe (1) a sudden shift of wind from northeast to southeast-south or southwest; (2) a belt of Cumulonimbus clouds

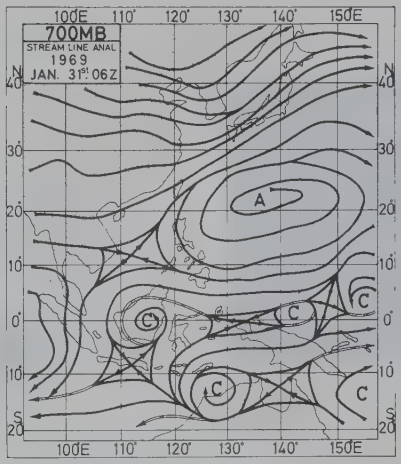

Fig. 24. Stream line at altitude 700 mb surface. 06Z. January 31, 1969.

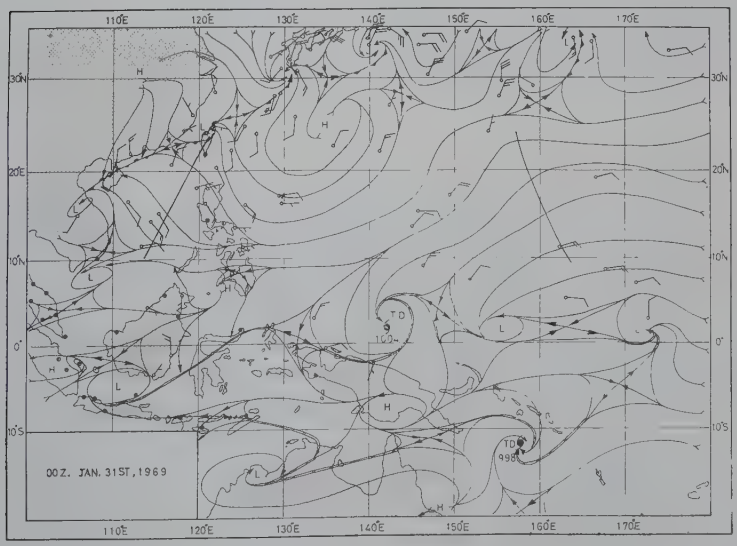

Fig. 25. Stream line at the surface. 00Z. January 31, 1969.

Fig. 26. The PPI echo picture shows the condition in the vicinity of the neutral corner accompanied with the ITC. 00Z. January 31, 1969. The position was lat. 3°N, long. 133°24′E.

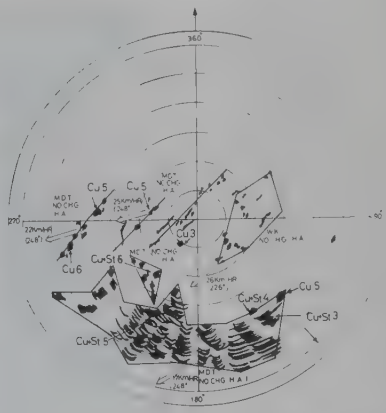

Fig. 27. The anlysis of the PPI echo picture in Fig. 20.

with showers, sometimes Altostratus cloud; (3) during periods of no convergence, no clouds and precipitation; (4) the rapid fall of temperature at the commencement of squall and lower temperature prevailing over the neighborhood waters (TSUROUKA and MATSUMOTO, 1965). However, there was no large change in temperature between both sides of the weak ITC.

7. Easterly wave

The disturbance in the tropical area probably occures by the horizontal convergence which is produced by the trades of both hemispheres, the Easterly wave, the ITC and the Polar trough. The disturbance frequently becomes a tropical cyclone. There are wave-shaped streamlines superimposed upon the easterly wind in the trades winds belt. The marked feature is that there is a low pressure trough poking northward into the trade winds, but no definite low pressue center. The winds are more or less uniform from the east-northeast and sky is fair with scatterd flat or modest cumulus clouds. The inversion in the trades is low, with moist air under it and dry subsided air aloft. While the wavy trough of pressure advances, the winds above the surface layer swings to a more northerly direction, the inversion layer rises suddenly, and the thickness of cloud become thicker. When it passes, showers develop and thunderstorms often are over. Sometimes, the showery and

squally weather continues for some time, but as the barometric wave progresses westward, the trades winds inversion lowers and the weather becomes fair again. However, on the tropical area, it seems that the phenomenon is just opposite. In another words, the weather continues to be fair before the passing of the wave and becomes a foul after that. There are Cumulus humlis, and haze, but no precipitation in front of the trough line.

On the other hand, in the area of the trough line, there are Cumulus congestus and Cumulonimbus with layers of Stratocumulus, Altostratus, Altocumulus and Cirrus. A moderate or heavy shower frequently occurs, and also, sometimes, it accompanies a light rain while showering. A weak low pressure center appears often at the vicinity of the Equator where we have the southern part of the North Equatorial Current. If the end of an easterly wave reaches the above mentioned low pressure, such a center of the low pressure may become occasionally a tropical cyclone (SHIBATA, 1965). The surface pressure change may be less than 1 mb when passing through wave.

8. Tropical cyclone and typhoon

On our three cruises we had two typhoons; one on Feburary 28, 1968 (HAYASHI, MIYASHITA and FUJITA; 1968) and the other Typhoon Phyllis in 1969. The track of tropical storm Phyllis is shown in Fig. 28. Tropical depression (1,000 mb) occurred at lat. 9°3′N, long. 166°E on January 17, 1969 and moved west-northwest or west. She developed rapidly and was called the tropical storm Phyllis at 18 GMT on January 17. The maximum wind speed was 60 knots (see Fig. 6 and 7). The minimum pressure was 965 mb. However, the detailes of the tropical storm were not clear, but its intensity became gradually weak ever since. Thus, she disappeared in the northeast of Samar Island of the Philippines. The sea surface temperature is higher where a tropical cyclone or a typhoon occurs than in the other area. The air temperature and dew poin temperature at the sea surface relates well with the sea surface temperature. The difference between the air temperature and the sea surface temperature along. 137°E in January in 1967, 1968 and 1969 is shown in Fig. 29.

A tropical cyclone or typhoon formed only in those waters away where the sea surface temperature was above 26°—27°C. A special interesting fact is that a weak tropical cyclone existed frequently in the vicinity of the Equator in long. 160°E. It seems that the sea surface temperature exceeds the critical value in this

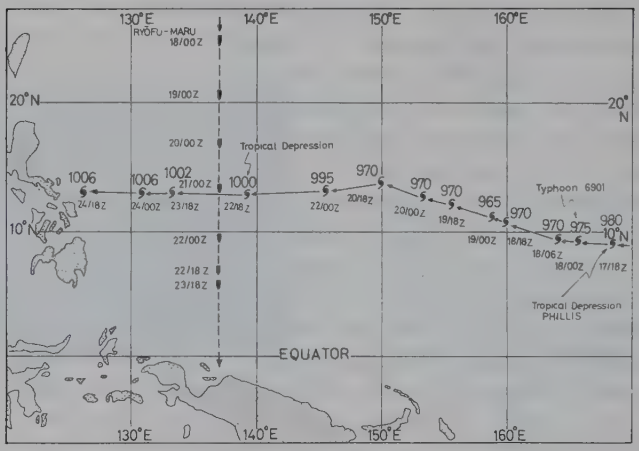

Fig. 28. The track of the tropical storm Phyllis and the course of R.V. *Ryofu Maru*.

area. According to our observations, all of the tropical cyclone or typhoon in this region move ordinarily westward, and as soon as they reach comparatively cold waters or subtropical region, they die out. They are sensitive to little variation of temperature or moisture. In the region where tropical cyclone normally forms, cyclogenesis may be impeded if the air temperature and the dew point temperature are below average or if the sea surface temperature is lower than normal. On account of these facts, the tropical cyclone probably generates easily under a fit condition over the southern part of the North Equatorial Current in the western North Pacific Ocean, because a convectional activity appears in low levels and amount of cloud is much or ceiling of cloud is lower than in the subtropical area. On the other hand, the condition of the sequence of cloud in high levels is akin to that we observed while warm front approached in the subtropical regions.

When tropical cyclone or typhoon moves westward in the tropical region, we shall experience that the sea-level pressure falls more than 3—3.5 mb/day or 5 mb/day, in the trades belt, we shall experience that the easterly wind with increased speed in a limited area should be suspected.

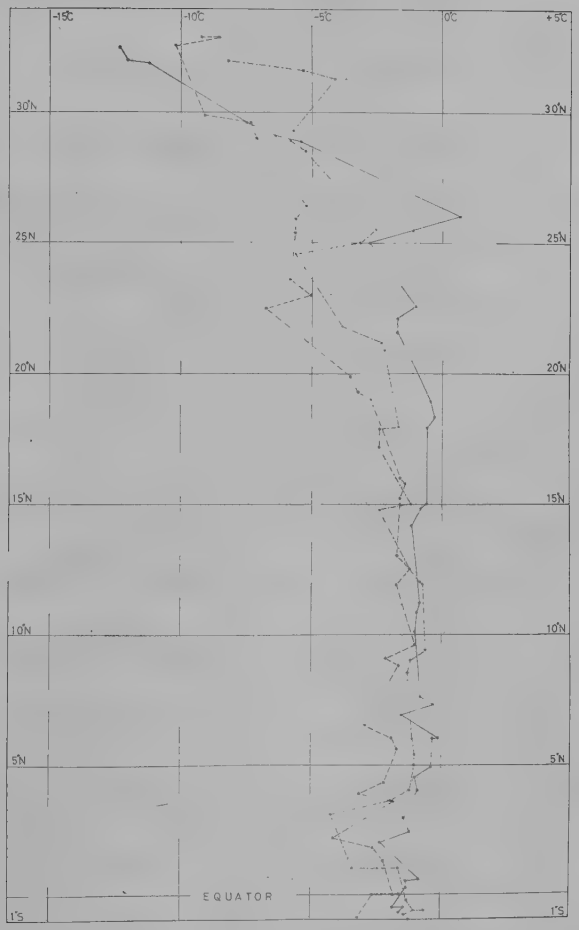

Fig. 29. The difference between air temperature and sea surface temperature along lat. 137°E in January of 1967, 1968 and 1969. When the sea surface temperature is higher than the air temperature, the value is shown with minus symbol. Solid line: 1969, Broken line: 1968, Dot-dash-line: 1967.

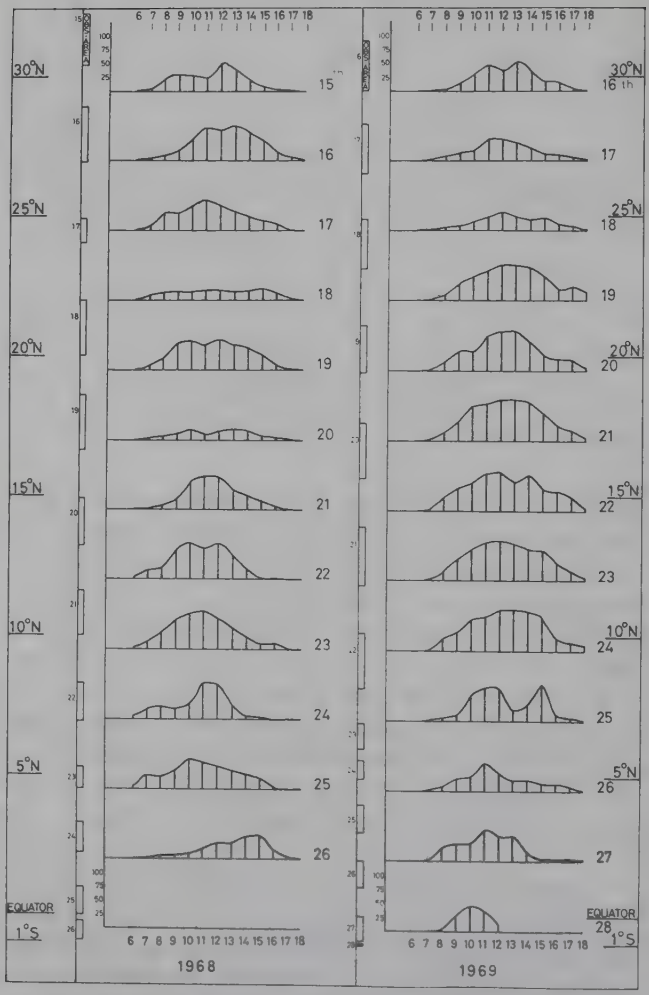

Fig. 30. The amount of global radiation along long. 137°E in 1968 and 1969. The unit is cal/cm²/hr.

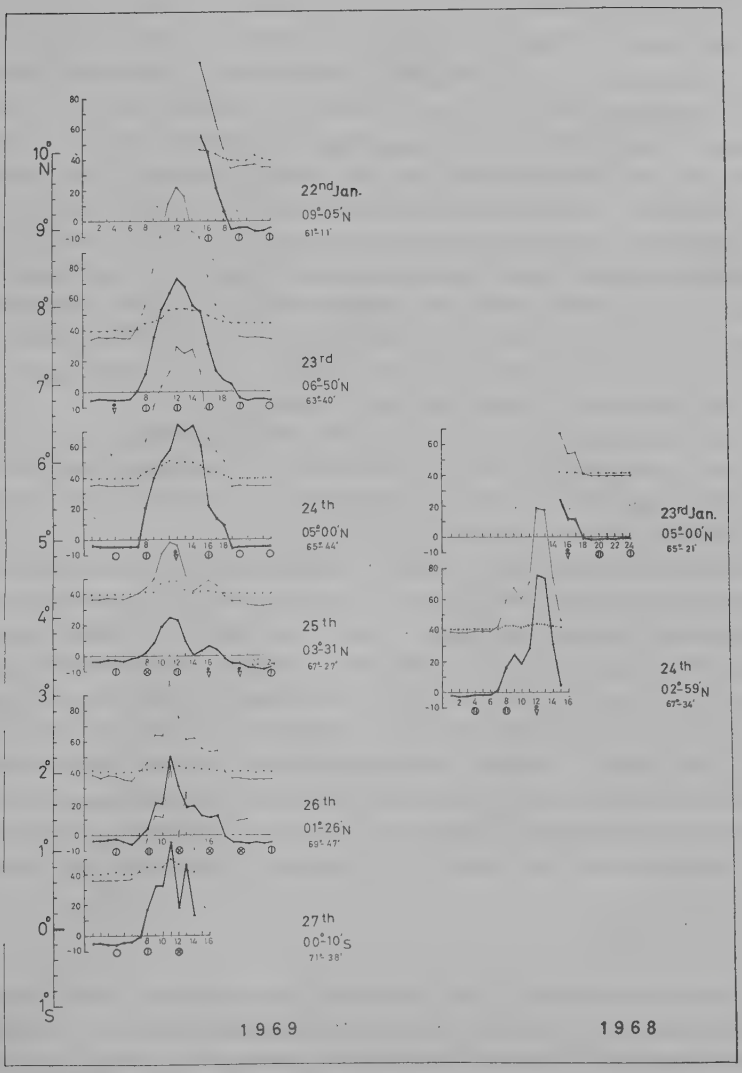

Fig. 31. Radiation balance along long. 137°E in 1968 and 1969.

9. Radiation

The observation of global radiation was carried out along lat. 137°E from the south coast of Japan to near the Equator in 1968 and 1969. Unfortunately, we could not always stop the ship, at a proper time for the observation and set up the instrument on suitable places on the ship. However, in the low latitudes we measured long and short waves radiation for a few days (Fig. 30 and 31). Figure 30 shows that the amount of downward radiation varies with latitude and the altitude of the sun; high near lat. 20°N, and low in the north and tropices. This distribution seems to be due to frequently travelling extratropical cyclones in the subtropical area and many Cumuliform clouds in the tropical area (Fig. 19). In our case, cloudness is generally small during night, but as soon as the sun rises, the Cumuliform cloud generates from place to place and Cumulus congestus or Cumulonimbus develops and then, there were scattered showers in the tropical area.

Let's compare with the values in the two years. The value near lat. 25°N in 1969 was small than in 1968. The distribution of radiation depends more upon weather's conditions than upon latitude. The maximum value was 69.6 cal/cm^2/hr on January 23, 1968 and 71.9 cal/cm^2/hr on January 21, 1969.

Now, according to Fig. 31, the observational area was just over the Equatorial Countercurrent, the decreasing tendency of the radiation balance was seen in the vicinity of the Equator. The reason is that the long and short waves of downward radiation decreased rapidly than in the other area and upward radiation did not change very much for all day. The average value of upward radiation by long wave was about 40 cal/cm^2/hr, it showed a little increasing tendency for the daytime. The amount of radiation balance decreased for the night and its value was minus, because the amount of downward radiation by long wave decreased a little and that of global radiation was zero. As the result of our analyses, it seems that the radiation balances are changed by the influence of the weather phenomena.

Acknowlegements

The author is grateful to the members of the scientific party, officers and crew aboard the *Ryufu Maru* for their cooperations throughout the survey. He wishes to express thanks to Dr. I. IMAI, Chief of Marine Department, to Mr. S. KAWAMURA, Chief of Maritime Meteorological Division, to Dr. J. MASUZAWA, to Mr. H. AKAMATSU, Chief scientists of these surveys and Mr. Y. KUGA, Marine Depertment, Japan

meteorological Agency for their useful suggestions and guidance in making this report, and to the Ryukyu Meteorological Observatory, to Taiwan Provincial Weather Bureau in the Republic of China, to Cebu Weather Bureau in the Philippines and to Royal Observatory in Hong Kong for their kind help.

References

Committee meeting of meteorological hand book: Meteorological hand book, pp. 1759 (in Japanese).

Herbert, R. (1954): Tropical meteorology. University of Chicago. pp. 392.

Hayashi, S., I. Miyashita and I. Fujita (1968): Maritime meteorological summary of western North Pacific Ocean in winter. *Oceanogr. Mag.* **20,** 105–120.

Petterssen, S. (1958): Introduction to meteorology. McGraw Company Inc. pp. 327.

Shibata, Y. (1965): Maritime meteorology and weather chart. Kaibundo Ltd, Tokyo, pp. 257 (in Japanese).

Tsuruoka, Y. and T. Matsumoto: General report of the participation of Japan in the International Indian Ocean Expedition. Science Council of Japan, pp. 133.

U.S. Navy: Marine climatic atlas of the world.
Vol. 2: North Pacific Ocean. (1958), pp. 175.
Vol. 3: Indian Ocean. (1957), pp. 267.
Vol. 5: South Pacific Ocean. (1959), pp. 276.

U.S. Navy: The pilot chart of weather summary for naval air pilot. New Guinea area. U.S. Hydrographic Office. pp. 108.

気象庁

欧文海洋報告

第 22 巻

THE OCEANOGRAPHICAL MAGAZINE

Vol. 22

Published by the Japan Meteorological Agency

1970

CONTENTS

MASUZAWA, J., T. AKIYAMA, Y. KAWARADA and T. SAWARA:
Preliminary report of the *Ryofu Maru* Cruise Ry 7001 in January-March 1970 1

MORIYASU, S.: On the change of monthly sea surface temperature
in the Western North Pacific (II) 27

IIDA, H.: Edge waves on the linearly sloping coast I. Free waves 37

SAGI, T.: On the distribution of nitrate nitrogen in the western
North Pacific Ocean 63

AKAMATSU, H.; The ocean data station buoys of the Japan
Meteorological Agency 75

HAYASHI, S., H. TAKANO and A. YAMASHITA: Maritime meteorological
summary of western North Pacific Ocean in the winters of 1967,
1968 and 1969 95

昭和46年3月31日　発行

編集兼
発行者　気象庁
東京都千代田区大手町1の3の4

印刷者　藤原秀雄

印刷所　昌美印刷株式会社
東京都千代田区神田錦町3の16